AD_____

Award Number: DAMD17-03-1-0006

TITLE: Disruption of Fibroblast Growth Factor Receptor (FGFR) Signaling as an Approach to Prostate Cancer Therapy

PRINCIPAL INVESTIGATOR: Mustafa Ozen, M.D., Ph.D.

CONTRACTING ORGANIZATION: Baylor College of Medicine
Houston, TX 77030

REPORT DATE: April 2006

TYPE OF REPORT: Final

PREPARED FOR: U.S. Army Medical Research and Materiel Command
Fort Detrick, Maryland 21702-5012

REPORT DOCUMENTATION PAGE

Form Approved
OMB No. 0704-0188

1. REPORT DATE *(DD-MM-YYYY)*	**2. REPORT TYPE**	**3. DATES COVERED** *(From - To)*
01-04-2006	Final	1 APR 2003 - 31 MAR 2006

4. TITLE AND SUBTITLE
Disruption of Fibroblast Growth Factor Receptor (FGFR) Signaling as an Approach to Prostate Cancer Therapy

5a. CONTRACT NUMBER

5b. GRANT NUMBER
DAMD17-03-1-0006

5c. PROGRAM ELEMENT NUMBER

6. AUTHOR(S)
Mustafa Ozen, M.D., Ph.D.

E-mail: mozen@bcm.tmc.edu

5d. PROJECT NUMBER

5e. TASK NUMBER

5f. WORK UNIT NUMBER

7. PERFORMING ORGANIZATION NAME(S) AND ADDRESS(ES)

Baylor College of Medicine
Houston, TX 77030

8. PERFORMING ORGANIZATION REPORT NUMBER

9. SPONSORING / MONITORING AGENCY NAME(S) AND ADDRESS(ES)
U.S. Army Medical Research and Materiel Command
Fort Detrick, Maryland 21702-5012

10. SPONSOR/MONITOR'S ACRONYM(S)

11. SPONSOR/MONITOR'S REPORT NUMBER(S)

12. DISTRIBUTION / AVAILABILITY STATEMENT
Approved for Public Release; Distribution Unlimited

13. SUPPLEMENTARY NOTES

14. ABSTRACT

Prostate cancer cells express multiple types of FGF receptor and increased expression of FGF receptor-1 (FGFR-1) is present in poorly differentiated human prostate cancers *in vivo.* We have proposed to evaluate biological affects of DN FGFR expression in human primary prostate epithelial cells and prostate cancer cell lines. The findings in this report support that prostate cancer cells are dependent upon FGFR signaling for survival and cells treated with DN FGFR are arrested G2/M phase of cell cycle followed by cell death. FGF signaling modulated *CDC25C* activity in prostate cancer, and in this manner can promote progression through the G2/M checkpoint. *CDC25C* protein is upregulated in comparison to normal prostate tissue and is present almost exclusively in its active dephosphorylated form. Determining other molecules involved in this pathway contributing tumor growth and survival will facilitate the development of cancer therapies to target FGF signaling pathway

15. SUBJECT TERMS
growth factors, fibroblast growth factors, fibroblast growth factor, Receptors, prostate cancer therapy, cell cycle

16. SECURITY CLASSIFICATION OF:			**17. LIMITATION OF ABSTRACT**	**18. NUMBER OF PAGES**	**19a. NAME OF RESPONSIBLE PERSON**
					USAMRMC
a. REPORT	**b. ABSTRACT**	**c. THIS PAGE**			**19b. TELEPHONE NUMBER** *(include area code)*
U	U	U	UU	30	

Table of Contents

INTRODUCTION:

Alterations in Fibroblast Growth Factor (FGF) signaling pathway have been implicated in the pathogenesis of variety of malignancies including prostate cancer by *in vitro* and *in vivo* studies[Polnaszek et al., 2003;Ozen et al., 2001;Takahashi, 1998;Giri et al., 1999]. FGFs produce their mitogenic and angiogenic effects in target cells by signaling through four distinct cell-surface tyrosine kinase receptors, FGFR-1 through FGFR-4. Prostate epithelial cells express FGF receptors and require FGFs for growth in primary culture. Prostate cancer cells express multiple types of FGF receptor and increased expression of FGF receptor-1 (FGFR-1) is present in poorly differentiated human prostate cancers *in vivo*[Takahashi, 1998;Giri et al., 1999]. We hypothesized that FGF receptor signaling is essential for viability of human prostate cancer cells and disruption of this signaling via expression of a dominant negative FGF receptor-1 protein in human prostate cancer cells might contribute to the death of cancer cells and can be used as adjuvant to current treatment options especially to radiotherapy since it has been also administered locally. Furthermore, analysis of gene expression profile in FGFR DN transfected cells might help our understanding of how FGFR DN works and the differentially expressed genes determined by microarray analysis can be used as targets for prostate cancer therapy.

BODY:

Task 1: We have proposed to evaluate biological affects of DN FGFR expression in human primary prostate epithelial cells and prostate cancer cell lines. We have obtained different recently established prostate cancer cell lines from other investigators and American Type Culture Collection (ATCC). Among these are 22Rv1[Sramkoski et al., 1999] obtained from ATCC, LAPC4 [Craft et al., 1999] from Dr. Charles Sawyers of University of California, Los Angeles, C4, C4-2 and C4-2B[Thalmann et al., 2000] from Dr. Leland Chung of University of Virginia and MDA PCa 2b [Navone et al., 1997] from Dr. Nora Navone of University of Texas M.D. Anderson Cancer Center. These cell lines have been frozen in liquid nitrogen for further experiments. Normal prostate biopsy specimens were also cultured for the purpose of obtaining primary prostate epithelial cells. All cell lines have been tittered for optimal multiplicity of infection (MOI) to be used in subsequent experiments. Viral particles was used to establish MOIs in cell lines since this has been suggested

Table1. Prostate cancer cell lines and appropriate MOIs used in adenovirus infection

Name of the cell line	Origin	Androgen Status	MOI used (in thousand particles)
DU145	Brain metastasis	insensitive	3
PC3	Bone metastasis	insensitive	4
LNCaP	Lymph node metastasis	sensitive	2.5
22 Rv1	CWR22R	insensitive	5
LAPC4	Bone metastasis	sensitive	2.5
MDA Pca 2b	Bone metastasis	sensitive	6
C4	LNCaP	insensitive	4
C4-2	LNCaP	insensitive	5
C4-2B	LNCaP	insensitive	5

as a reliable approach in the literature [Green et al., 2002;Yotnda et al., 2002]. This data and the phenotypes of the cell lines are summarized in Table 1.

To analyze the affect of DN FGFR in human prostate cell proliferation and/or viability, cells were counted by Coulter counter after 24, 48 and 72 hr of infection with DN FGFR and LacZ. As seen in Figure 1, LAPC4 cells had the most dramatic effect on the inhibition of cell proliferation when infected with DN FGFR adenovirus. Over 90 % of the cells died after 72 hours of infection with DN FGFR; however, there was a 16% increase on the number of cells infected with LacZ as control. MDA Pca 2b cells also showed decreased in the number of proliferating cells after infection with DN FGFR adenovirus as compared to control at all three time points (Figure 1). After 72 hours of infection cells treated with DN FGFR stopped proliferating as contrast to the cells infected with control adenovirus which continued to grow and more than doubled in number in 72 hours. The 22 Rv1 cell line only had significant reduction on the number of proliferating cells after 72 hours of infection.

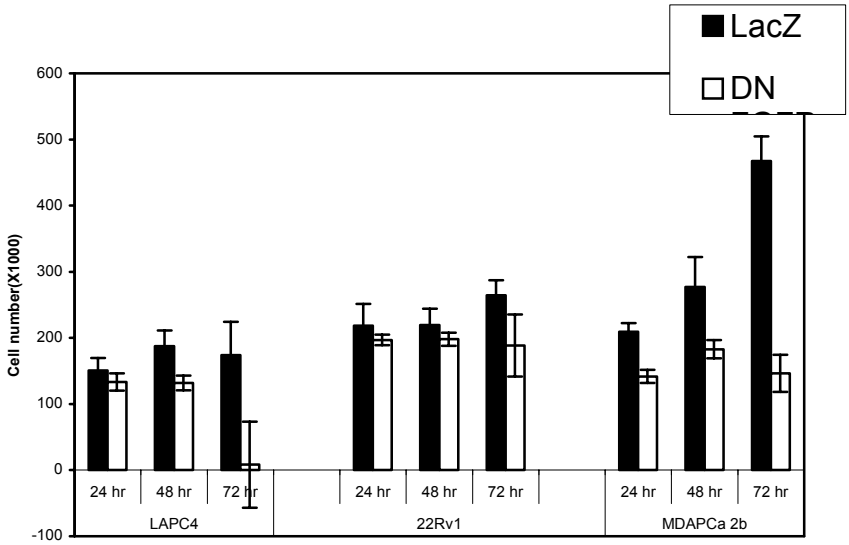

Figure 1. Effect of DN FGFR on prostate cancer cell proliferation and viability. LAPC4 22Rv1 and MDA PCa 2b cells were plated at 5 x 10^4 cells per 35-mm dish and infected with Ad FGFR or Ad Lac Z as control. The cell number was determined by counting with the use of Coulter counter at 24, 48, and 72 hours after infection. All values are the mean of triplicate determinations.

A series of lineage-related LNCaP cell sublines that reflect the various steps of prostate carcinogenesis and progression has been derived[Thalmann et al., 2000]. An androgen-independent (AI) cell line, C4-2, reproducibly and consistently follows the metastatic patterns of hormone-refractory prostate cancer by producing lymph node and bone metastases when injected either s.c. or orthotopically in either hormonally intact or

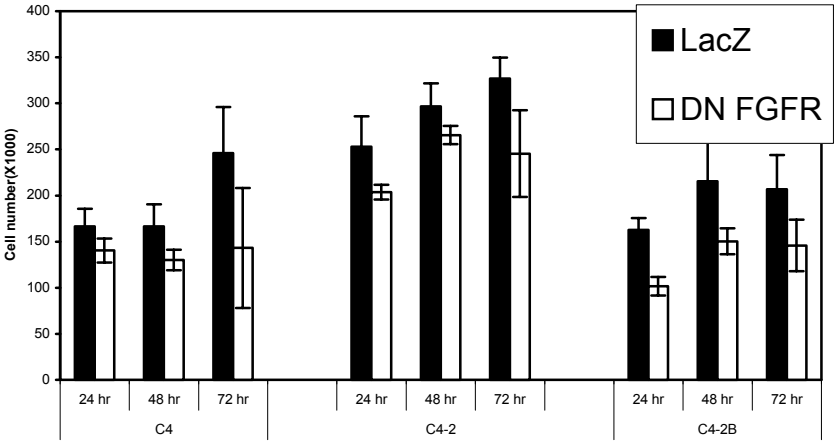

Figure 2. Effect of DN FGFR on prostate cancer cell proliferation and viability on LNCaP prostate cancer sublines C4, C4-2 and C4-2B.

castrated hosts[Thalmann et al., 2000]. This LNCaP model will help improve our understanding of the mechanisms of androgen-dependent to androgen-independent prostate cancer progression. As seen on Figure 2, although DN FGFR adenovirus treatment did decrease the proliferation of all three LNCaP derivatives, The biological effect was not as dramatic as it was in parental LNCap cells. We have previously observed 50- 70% decrease in cell number by 72 hours after DN FGFR treatment [Ozen et al., 2001]. One possible explanation of this difference could be the difference in the endogenous FGF2 responds to the DN FGFR treatment of these cell lines. This possibility is currently under investigation. It is interesting, however, to note that the original LNCaP cell line was androgen sensitive in contrast to C4-2 sub-lines. Two of the cell lines, LAPC4 and MDA PCa 2b, mentioned earlier to have the most biological effect after DN FGFR treatment are also androgen sensitive prostate cancer cell lines. It might be interesting to test the effect of DN FGFR on different androgen sensitivity conditions.

For the examination of the effect of the DN FGFR on cell cycle progression, prostate cells were infected with AdDN FGFR and AdLacZ and flow cytometry analysis was performed after different time points (24, 48 and 72 hours). A summary of these results is shown in Figures 3 A and B.
All cell lines tested except C4-2 accumulated in G2/M 72 hours after the infection with DN FGFR. In 48 hours of infection with DN FGFR, C4-2 cells, however showed 20% increase in the number of cells in G2/M phase. The accumulation of cells in G2/M did not correlate the biological effect of DN FGFR in every cell line. For example, treatment of DN FGFR showed more biological effect on MDA PCa 2b cells as compared to 22Rv1 cells after 72 hours of infection (28% reduction in cell number after 72 hours of infection in 22Rv1 cells vs

A.

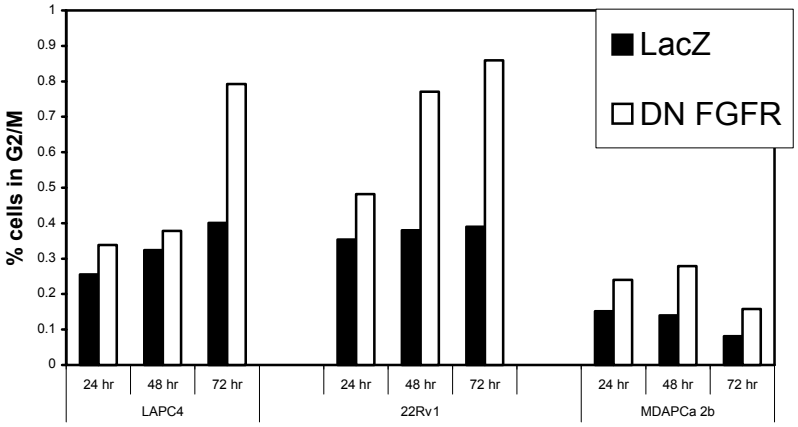

B.

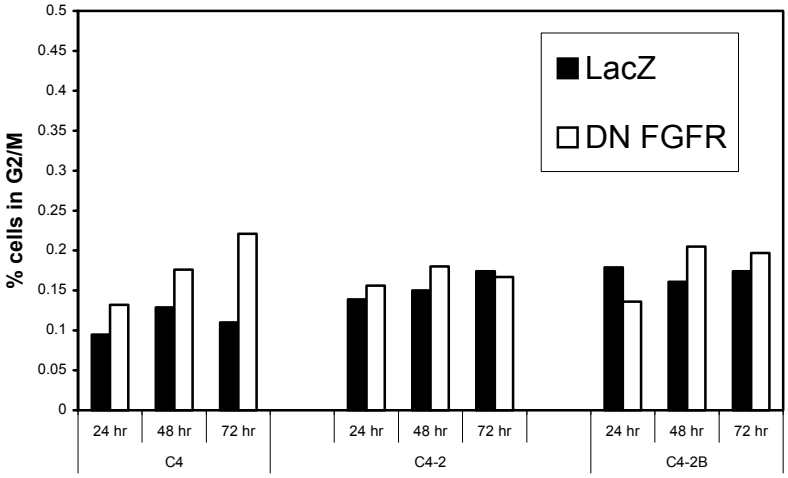

Figure 3. Prostate cancer cells, LAPC4, 22Rv1 and MDA Pca 2b (A) and C4, C4-2 and C-42B (B) were infected with AdDN FGFR and AdLacZ and flow cytometry analysis was performed after 24, 48 and 72 hours. Percent of the cells in G2 is shown in each on the y-axis.

68% reduction in MDA PCa 2b cells). However, The percentage of the cells in G2/M were 85 and 15 in 22 Rv1 and MDA PCa cells, respectively. This might require further investigation. 22 Rv1 cells might need more time to acquire the biological effect of DN FGFR. Cell cycle analysis of DN FGFR treated LAPC4 cells as a representation is shown in Figure 4.

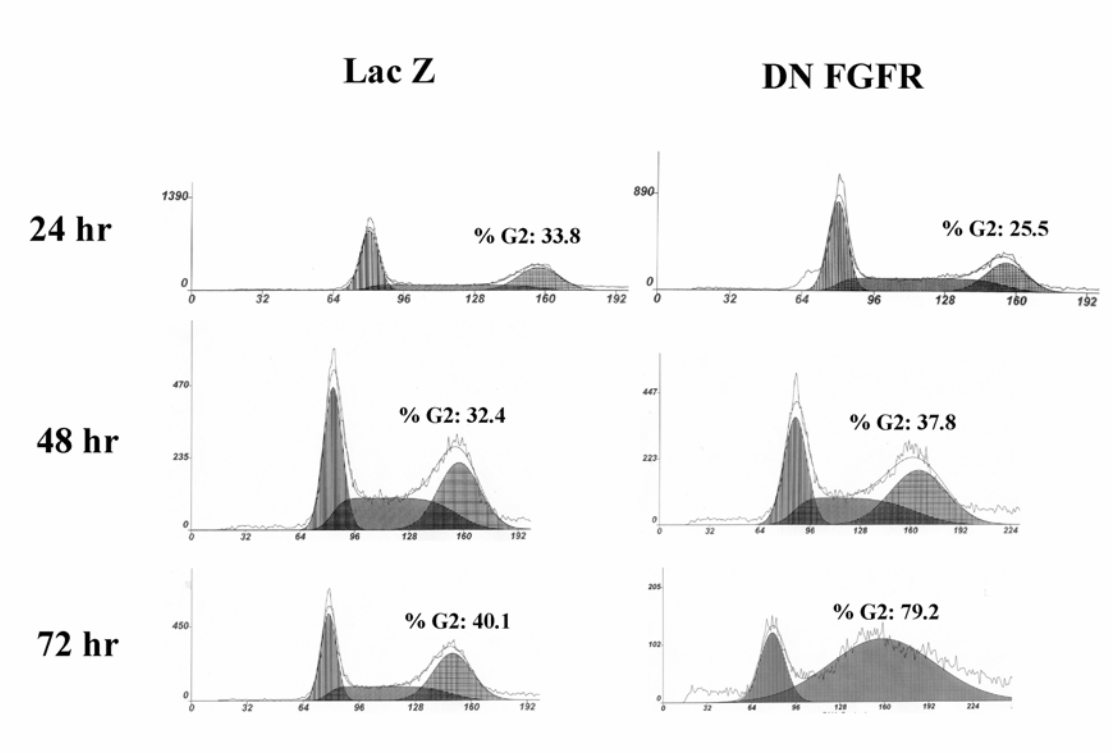

Figure 4. Cell cycle analysis of DN FGFR infected LAPC4 cells. In each case, cell number is represented on the y-axis, with the corresponding fluorescence at 550 nm is shown on the x-axis. Flow cytometry data are seen as a line, and filled area represents the result of cell cycle analysis by the use of Multi Cycle software. The percantage of G2/M as determined with this software is indicated.

Since the production of our original AdDN FGFR, further developments have been made in the area of adenoviral delivery to enhance the transduction ability of the vectors such as Ad5 and Ad35. The entry pathway for Ad5 consists of initial binding to the cell, which is mediated by the association of the Ad5 fiber protein and a 46-kd membrane protein called CAR, followed by internalization. CAR is a member of the immunoglobulin superfamily

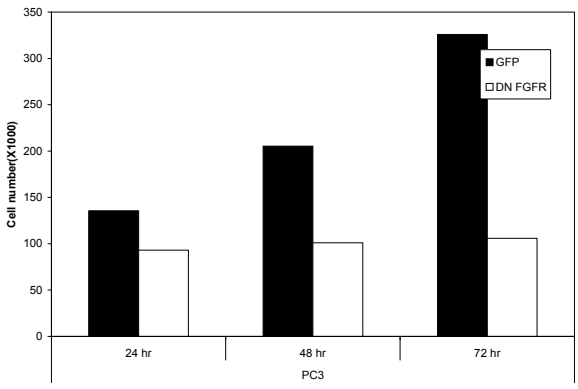

Figure 5. Effect of DN FGFR on cell proliferation and viability of PC3 prostate cancer cell line.

and also serves as the receptor for coxsackie B virus. Recently, a new adenovirus vector has been developed in which the fiber protein of adenovirus type 35 (Ad 35) has been substituted for the fiber protein of Ad5 that allows the virus to enter cells in a CAR-independent fashion. It has been shown that this new vector could efficiently transfer genes into hematopoietic stem cells and human bone marrow mesenchimal stem cells[Yotnda et al., 2001;Olmsted-Davis et al., 2002a;Shayakhmetov et al., 2000]. With the collaboration of our colleagues Drs. Elizabeth Olmsted-Davis and Alan Davis of Vector Development Core Facility at our Institution, we were able to construct Ad5F35 DN FGFR. This new adenovirus is highly efficient on affecting all the cell lines used. We were able to get efficient infection on PC3 cell line that has been failed to get infected with the previous adenovirus. Figure 5 shows the affect of the new adenovirus on PC3 cell proliferation.

Fortunately, we obtained a monoclonal antibody from Biodesign International, Inc. (Saco, ME) detecting extracellular domain of FGFR1. This antibody reacts with both alpha (denatured) and beta isoforms and the epitope is within the sequence his241 and val267 between Ig loops II and III. By using this antibody after titration for our experiments, we easily can show the successful infection of cells with AdDN FGFR. Figure 6 shows the detection of DN FGFR on Western blots. As seen in this figure DN FGFR infected PC3 cells showed a strong band, corresponding to DN FGFR protein, on a Western blot incubated with the new FGFR1 antibody, suggesting successful infection efficiency on PC3 cells after 24 hr time point. This data is verified in all cell lines used.

Figure 6. Detection of DN FGFR protein in AdDN FGFR treated cells.

Task 2: We proposed to investigate the growth inhibitory ability of DN FGFR in prostate cancer xenografts. Total of 35 Athymic NCr-nu/nu male homozygos 6-8 week-old nude mice were purchased from Charles Rivers Laboratory. Three way Differential Reactive Stroma (DRS) Xenograft tumors were generated as originally described by Tuxhorn et al.[Tuxhorn et al., 2002] 2 x106 LNCaP cells and 0.5X106 stromal cells were mixed with Matrigel and injected in each lateral flank of animal. Stromal cells were provided by Dr. David Rowley, from the department of Molecular and Cellular Biology of our Institution. Five animals (10 injection site) were used for each experiment set. A total of three sets for each of the DN FGFR and gfp infection are used. In one group when the tumor

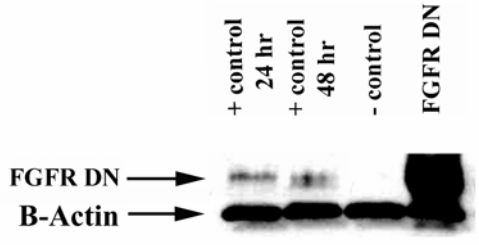

Figure 7. Detection of DN FGFR protein in AdDN FGFR treated xenografts.

reached 0.5 mm in size AdDN FGFR is injected intratumorally. One animal was sacrificed after two rounds of injection to verify successful delivery of DN FGFR. The tumor lysed in lysis buffer and the lysate subjected to Western blot experiments by using FGFR1 antibody described above. As seen in Figure 7, DN FGFR injected tumor showed remarkable expression of DN FGFR protein. We were able to generate 51 three way xenografts using LNCaP+Matrigel+stromal cells in 27 animals. Among these, 26 and 25 tumors were treated with AdGFP and AdDN FGFR, respectively. The treatment was carried out every five days in at least 3 cycles. As can be seen in Figure 8, in AdDN FGFR treated group, the number of tumors detectable at the end of the experiment was significantly low as compared to control group treated with AdGFP (13 out of 26 detectable tumors in AdDN FGFR vs 23 out of 25 detectable tumors in AdGFP). The mean tumor size was reduced 54% in AdDN FGFR treated group although the mean tumor size was increased 2.4 fold in control group (Figure 8). The results from these *in vivo* experiments are being prepared as a manuscript.

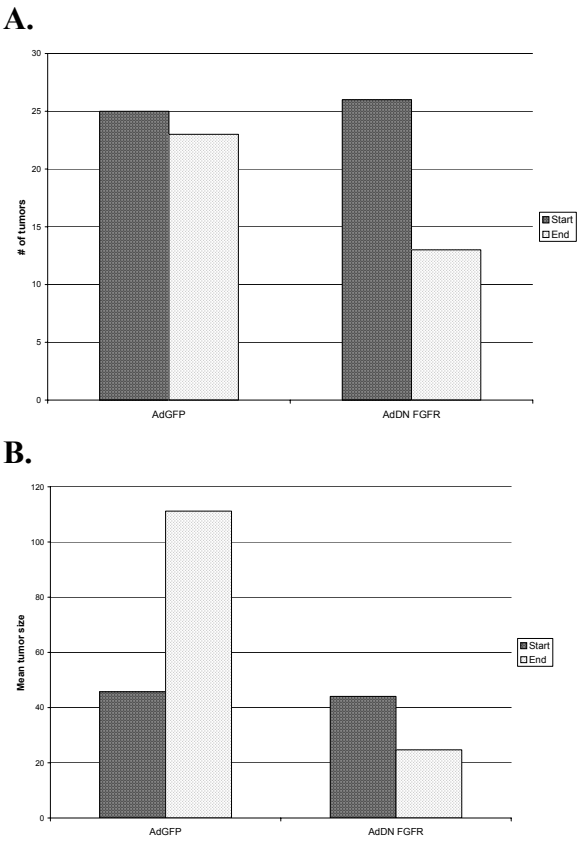

Figure 8. The results of in vivo experiments. The tumors treated with either AdDN FGFR or AdGFP as control. The number of tumors detectable (A) and the mean tumor sizes (B) are shown.

Task 3: In this task, we proposed to identify and cluster the differentially expressed genes in FGFR DN treated and untreated cells by microarray analysis across prostate cancer cell lines. In our preliminary experiments one of the differentially expressed genes in AdDN FGFR treated cells was CDC25C. CDC25 phosphatases belong to the tyrosine phosphatase family and play a critical role in regulating cell cycle progression by dephosphorylating cyclin dependent kinases at inhibitory residues. In human cells, cdc25 proteins are encoded by a multigene family, consisting of *CDC25A*, *CDC25B*, and *CDC25C[Hoffmann, 2000;Turowski et al., 2003]*. In late G2, the *CDC25C* dephosphorylates Cdc2 on both threonine 14 and tyrosine 15, leading to the activation of Cdc2/cyclin B complexes[Graves et al., 2001;Dunphy and Kumagai, 1991;Strausfeld et al., 1991] and progression through the G2/M checkpoint. Phosphorylation of serine 216 of *CDC25C* throughout interphase and upon G2 checkpoint activation has been found to negatively regulate the enzymatic activity of *CDC25C* [Graves et al., 2000;Peng et al., 1997] and a positive feedback loop has been proposed between cdc2 and *CDC25C* [Hoffmann,

2000;Peng et al., 1997;Izumi and Maller, 1995;Strausfeld et al., 1991]. Activated Chk kinases can inactivate *CDC25C* via phosphorylation at serine 216, blocking the activation of cdc2 and transition into M-phase [Zeng et al., 1998]. Another aspect of Cdc25 regulation is alternative splicing that may produce at least five *CDC25B* variants [Baldin et al., 1997]. Splice variants are also reported for *CDC25A* and *C* [Wegener et al., 2000;Bureik et al., 2000]. The activity and regulation of *CDC25C* in prostate carcinoma has not been previously examined, despite its potentially important role in the G2/M transition in this common malignancy. To determine whether *CDC25C* plays a role in prostate cancer, we have examined the expression of *CDC25C* and its alternatively spliced variant in human prostate cancer. *CDC25C* protein is upregulated in comparison to normal prostate tissue and is present predominantly in its active dephosphorylated form. In addition, expression of a biologically active alternatively spliced *CDC25C* isoform is increased in prostate cancer. In addition, we have found, by expression of dominant negative fibroblast growth factor (FGF) receptors, that FGF signaling modulated *CDC25C* activity in prostate cancer, and in this manner can promote progression through the G2/M checkpoint.

This study on CDC25C was presented in tenth Annual Meeting of Association of Molecular Pathology and the abstract was published in the Journal of Molecular Diagnostics. The full length manuscript entitled “Increased expression and activity of CDC25C phosphatase and an alternatively spliced variant in prostate cancer” is in press in Clinical Cancer Research. Copies of accepted manuscript, published abstract and the letter of acceptance are attached.

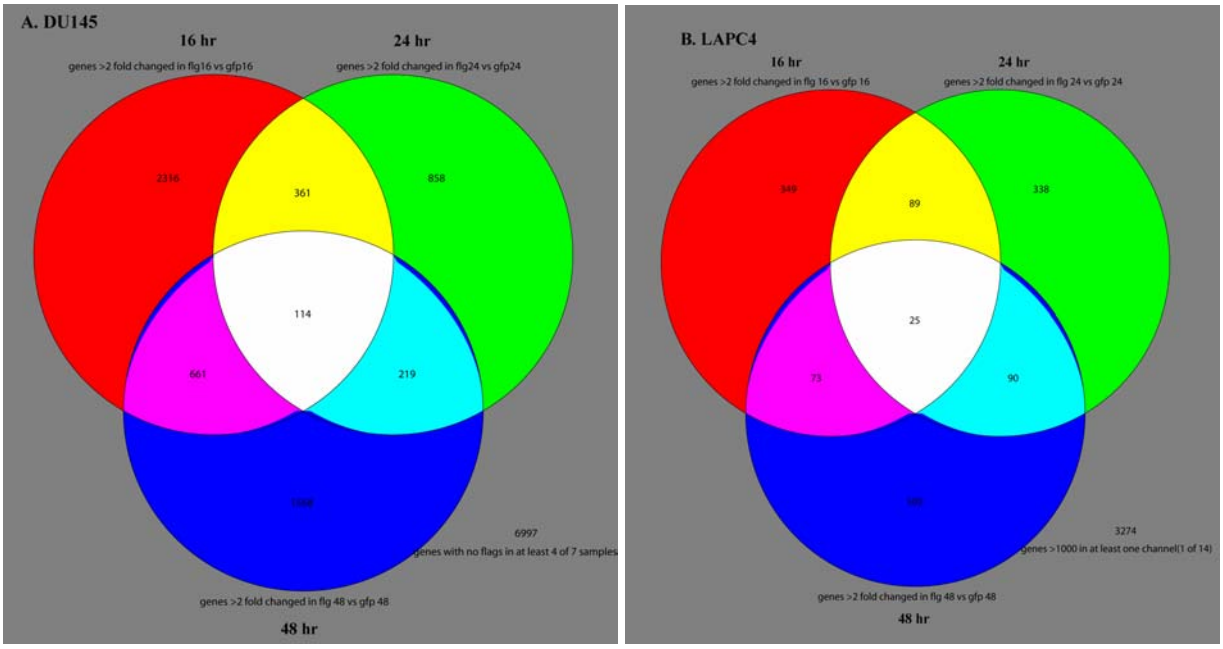

Figure 8. Summary of differentially expressed genes in DU145 (A) and LAPC4 (B) cell lines. The numbers of at least 2 fold differentially expressed genes are given inside the circles.

We have compared DU145 and LAPC4 cell lines treated with either gfp or DN FGFR carrying adenovirus in 16, 24, 48 and 72 hour time points. After hybridization and initial analysis, all data points were loaded to Gene Spring Software for further detail analysis. Microarray chip carrying oligonucleotides representing over 21 thousand human genes and transcripts obtained from Vancouver Microarray Core Facility (Vancouver, BC) were used. Data with low signal intensity, high background and high variability were eliminated. Array-specific data normalization was then performed using the LOWESS, "locally-weighted regression and smoothing scatter plots", procedure. Signals with raw intensity of less than 1000 in over half of the samples were also eliminated. The fold difference of the samples over the reference of these genes were calculated and grouped as they had over two fold differentially expressed values. Figure 8 shows the number of differentially expressed genes in DU145 cells in 8A and LAPC4 cells in 8B.

We have clustered these differentially expressed genes in all time points as seen in Figure 9. Gene annotations for these transcripts are given in Table 2.

A. DU145

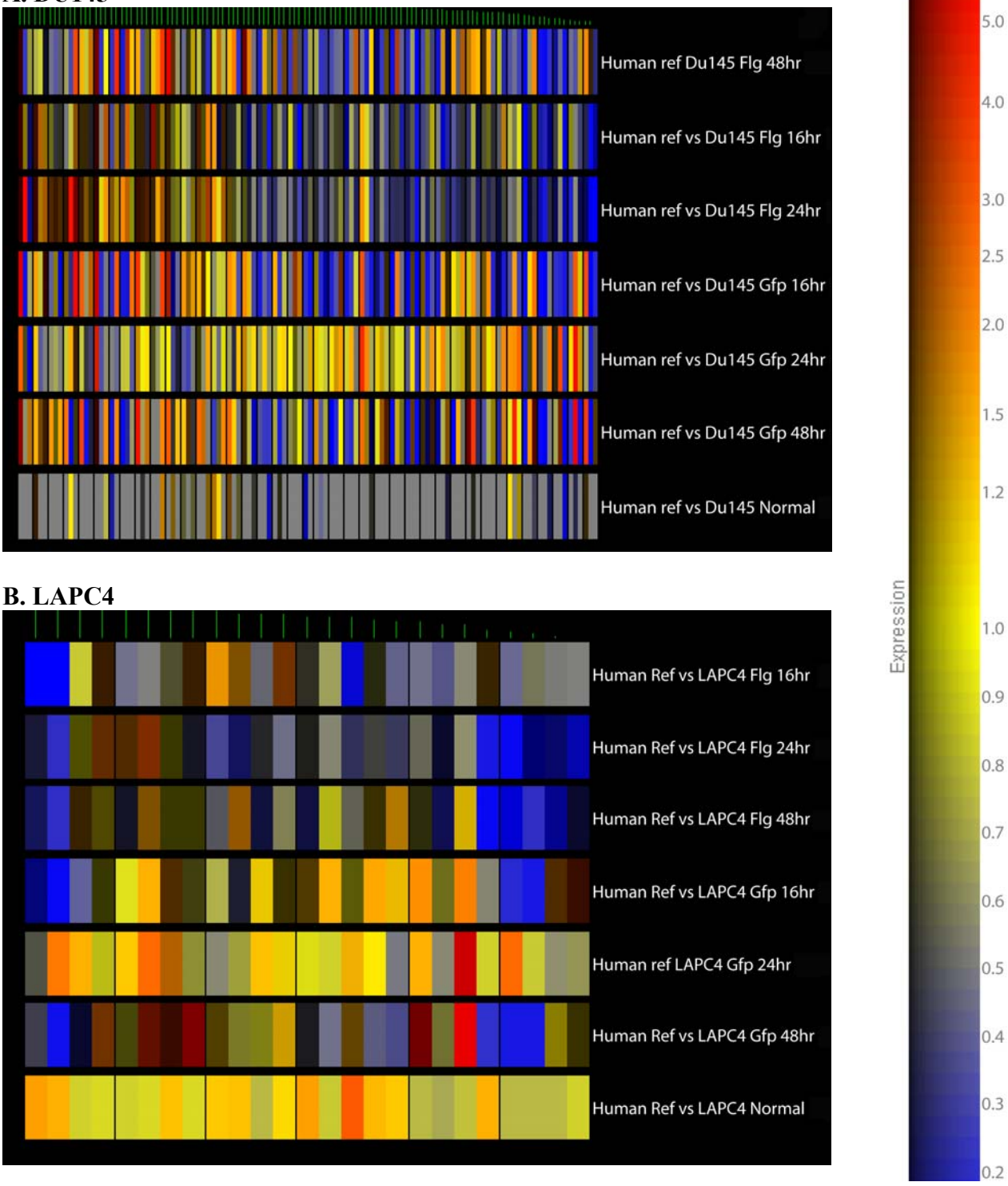

B. LAPC4

Figure 9. Clustering of the genes differentially expressed at least two folds at all time points in DU145 (A) and LAPC4 (B) cell lines. Each row represents a single sample and each column a single transcript. Each bar is colored by its expression at a given point as shown.

Table 2. Description of the genes differentially expressed in DU145 cells at all time points.

Fold change	Gene Description
12.76	Normal mucosa of esophagus specific 1^NMES1^NM_032413^112242^H2
7.523	Ras homolog gene family, member B^ARHB^NM_004040^204354^H200014
5.586	Homo sapiens cDNA FLJ14091 fis, clone MAMMA1000266^N/A^AK024153
5.378	Tyrosine 3-monooxygenase/tryptophan 5-monooxygenase activation
4.457	Homo sapiens cDNA FLJ25184 fis, clone CBR09423^N/A^AK057913^101
4.342	Homo sapiens cDNA FLJ14088 fis, clone MAMMA1000227^N/A^AK024150
4.239	Hypothetical protein FLJ10508^FLJ10508^NM_018118^274284^H200017
4.146	Likely homolog of mouse p140^KIAA1684^AB051471^278639^H20001733
4.104	PR domain containing 7^PRDM7^NM_052996^278234^H200017242
3.794	Homo sapiens, clone IMAGE:4851821, mRNA^N/A^BC015002^348705^H20
3.687	Centaurin, beta 1^CENTB1^NM_014716^108947^H200011613
3.498	Homo sapiens cDNA FLJ31060 fis, clone HSYRA2000925^N/A^AK055622
3.231	Homer, neuronal immediate early gene, 1B^SYN47^NM_004272^337737
3.191	Fibrillin3^KIAA1776^NM_032447^116265^H200012003
3.17	Homo sapiens cDNA FLJ11709 fis, clone HEMBA1005133^N/A^AK021771
3.15	Thyroid transcription factor 1^TITF1^U33749^197764^H200014771
2.99	Small inducible cytokine subfamily C, member 1 (lymphotactin)^S
2.982	Homo sapiens cDNA FLJ12209 fis, clone MAMMA1000962^N/A^AK022271
2.968	Homo sapiens mRNA full length insert cDNA clone EUROIMAGE 99418
2.819	Exonuclease 1^EXO1^NM_003686^47504^H200004844
2.815	Apolipoprotein M^G3A^NM_019101^247129^H200015859
2.814	ESTs, Moderately similar to located at OATL1 [H.sapiens]^N/A^BG
2.754	Putative UDP-GalNAc:polypeptide N-acetylgalactosaminyltransfera
2.736	Aryl hydrocarbon receptor nuclear translocator-like^ARNTL^NM_00
2.725	Hypothetical protein FLJ14494^FLJ14494^NM_032795^322406^H200018
2.689	Homo sapiens cDNA FLJ11599 fis, clone HEMBA1003879^N/A^AK021661
2.525	Homo sapiens putative ion channel protein CATSPER2 (CATSPER2),
2.505	Homo sapiens, clone IMAGE:4696946, mRNA, partial cds^N/A^BC0178
2.488	Homo sapiens mRNA; cDNA DKFZp586B0918 (from clone DKFZp586B0918
2.453	Lengsin^LGS^NM_016571^149585^H200013668
2.367	Hypothetical protein MGC20496^MGC20496^NM_052845^12106^H2000020
2.32	Carboxylesterase 2 (intestine, liver)^CES2^NM_003869^282975^H20
2.313	Ubiquitin-conjugating enzyme E2G 2 (UBC7 homolog, yeast)^UBE2G2
2.226	Homo sapiens mRNA full length insert cDNA clone EUROIMAGE 49248
2.209	ATP-dependent RNA helicase^ROK1^AK001652^99423^H200010964
2.179	Major histocompatibility complex, class I, F^HLA-F^NM_018950^11
2.169	Homo sapiens cDNA FLJ32921 fis, clone TESTI2006872^N/A^AK057483
2.164	Heterogeneous nuclear ribonucleoprotein H1 (H)^HNRPH1^NM_005520
2.157	Chemokine (C-X-C motif) ligand 16^CXCL16^NM_022059^82407^H20000
2.114	Homo sapiens cDNA FLJ31052 fis, clone HSYRA2000629, weakly simi
2.078	Hypothetical protein R33729_1^R33729_1^Z78330^10927^H200010095
2.049	KIAA1902 protein^KIAA1902^AB067489^7149^H200001372
2.007	Regulator of G-protein signalling 2, 24kD^RGS2^NM_002923^78944^
0.5	Interleukin 19^IL19^NM_013371^71979^H200005769
0.497	Hypothetical protein FLJ13593^FLJ13593^NM_024780^145807^H200013
0.497	Apolipoprotein L, 6^APOL6^NM_030641^257352^H200016431
0.494	CD37 antigen^CD37^NM_001774^153053^H200013851
0.491	Hypothetical protein FLJ21841^FLJ21841^NM_024609^29076^H2000038
0.487	Ribonuclease 6 precursor^RNASE6PL^AK001769^8297^H200001633
0.486	KIAA0770 protein^KIAA0770^BC015817^9452^H200001780
0.485	Retinoblastoma binding protein 5^RBBP5^NM_005057^72984^H2000058
0.473	Amplified in osteosarcoma^OS-9^AL137691^76228^H200006266
0.473	Rho GTPase activating protein 9^ARHGAP9^NM_032496^19807^H200002
0.466	Hypothetical protein FLJ10521^FLJ10521^NM_018125^116385^H200012

0.465	Homo sapiens cDNA FLJ30018 fis, clone 3NB692000529^N/A^AK054580
0.457	YDD19 protein^YDD19^U82319^350967^H200020967
0.449	Nuclear factor (erythroid-derived 2), 45kD^NFE2^NM_006163^75643
0.447	Low density lipoprotein receptor-related protein 4^LRP4^AB01154
0.444	DnaJ (Hsp40) homolog, subfamily C, member 3^DNAJC3^NM_006260^96
0.444	A disintegrin and metalloproteinase domain 11^ADAM11^NM_002390^
0.443	B7 protein^B7^NM_006992^155586^H200014095
0.442	Homo sapiens mRNA; cDNA DKFZp434G015 (from clone DKFZp434G015)^
0.438	Homo sapiens cDNA FLJ31499 fis, clone NT2NE2005441, weakly simi
0.432	Sprouty homolog 4 (Drosophila)^SPRY4^NM_030964^285814^H20000884
0.431	Kelch-like ECH-associated protein 1^KIAA0132^NM_012289^57729^H2
0.431	Receptor tyrosine kinase-like orphan receptor 2^ROR2^NM_004560^
0.43	Similar to RIKEN cDNA 1110002C08 gene^MGC9564^AK054669^343553^H
0.424	Homo sapiens mRNA for WNT14B, complete cds^N/A^NM_003396^350957
0.424	Kruppel-like factor 16^KLF16^NM_031918^303194^H200018168
0.41	Homo sapiens clone 23900 mRNA sequence^N/A^AF038184^293407^H200
0.406	Egf-like module containing, mucin-like, hormone receptor-like s
0.405	ESTs^N/A^AA278251^173345^H200014184
0.404	Homo sapiens cDNA: FLJ21572 fis, clone COL06651^N/A^AK025225^15
0.4	Matrix Gla protein^MGP^NM_000900^279009^H200017417
0.399	KIAA0610 protein^KIAA0610^AB011182^118087^H200012082
0.398	Homo sapiens cDNA FLJ25057 fis, clone CBL04590^N/A^AK057786^351
0.396	Hypothetical protein DKFZp762A227^DKFZp762A227^AL157431^274453^
0.395	Homeo box 11 (T-cell lymphoma 3-associated breakpoint)^HOX11^M6
0.388	Insulin-like growth factor 2 (somatomedin A)^IGF2^NM_000612^349
0.379	G protein-coupled receptor 23^GPR23^NM_005296^27812^H200003795
0.36	Protein tyrosine phosphatase, non-receptor type 7^PTPN7^NM_0028
0.359	Protein tyrosine phosphatase, receptor type, N polypeptide 2^PT
0.353	Tumor suppressing subtransferable candidate 4^TSSC4^NM_005706^1
0.353	Homo sapiens cDNA FLJ14130 fis, clone MAMMA1002618^N/A^AK024192
0.35	KIAA0825 protein^KIAA0825^AB020632^194755^H200014678
0.347	CGI-35 protein^LOC51077^NM_015962^343173^H200019907
0.338	Homo sapiens cDNA: FLJ21909 fis, clone HEP03834^N/A^AK025562^18
0.334	Hypothetical protein FLJ10477^FLJ10477^NM_018105^7432^H20000143
0.325	Sirtuin silent mating type information regulation 2 homolog 5 (
0.318	STE20-like kinase^JIK^AF181985^12040^H200002056
0.31	Cholecystokinin B receptor^CCKBR^NM_000731^203^H200000057
0.305	Homo sapiens cDNA FLJ25027 fis, clone CBL02392^N/A^AK057756^915
0.299	V-ets erythroblastosis virus E26 oncogene homolog 1 (avian)^ETS
0.295	Homo sapiens HSPC285 mRNA, partial cds^N/A^AF161403^293815^H200
0.285	Apelin; peptide ligand for APJ receptor^APELIN^NM_017413^303084
0.284	Homo sapiens mRNA; cDNA DKFZp586K1922 (from clone DKFZp586K1922
0.264	H2B histone family, member N^H2BFN^NM_003527^151506^H200013772
0.253	Homo sapiens cDNA FLJ30785 fis, clone FEBRA2000901^N/A^AK055347
0.25	H2A histone family, member K, pseudogene^H2AFKP^Z80777^334456^H
0.244	Short-chain alcohol dehydrogenase family member^HEP27^NM_005794
0.23	KIAA0211 gene product^KIAA0211^NM_014630^79347^H200006670
0.2	Homo sapiens clone CDABP0095 mRNA sequence^N/A^AY007155^46919^H
0.193	Carbamoyl-phosphate synthetase 1, mitochondrial^CPS1^NM_001875^
0.191	Follistatin^FST^NM_006350^9914^H200001854
0.174	BCL2-associated X protein^BAX^NM_004324^159428^H200007440
0.157	Homo sapiens mRNA full length insert cDNA clone EUROIMAGE 36278
0.154	Solute carrier family 18 (vesicular acetylcholine), member 3^SL
0.138	GATA binding protein 3^GATA3^NM_002051^169946^H200007883
0.126	Nuclear receptor binding protein^NRBP^NM_013392^272736^H2000169
0.0971	Protocadherin 1 (cadherin-like 1)^PCDH1^NM_032420^79769^H200006
0.0916	Homo sapiens mRNA; cDNA DKFZp564O0862 (from clone DKFZp564O0862
0.0912	Hypothetical protein FLJ20718^FLJ20718^NM_017939^50579^H2000049

Table 3. Description of the genes differentially expressed in LAPC4 cells at all time points. Only 24 hr time point fold change is shown.

Fold change	Gene Description
9.845	Hepatic leukemia factor^HLF^M95585^250692^H200016237
7.326	Annexin A5^ANXA5^NM_001154^300711^H200009920
2.539	WAS protein family, member 2^WASF2^NM_006990^347375^H200020128
2.462	Estrogen receptor binding site associated, antigen, 9^EBAG9^NM_
2.31	Putative 47 kDa protein^LOC56899^AF145204^92927^H200010556
2.162	Synaptogyrin 2^SYNGR2^NM_004710^5097^H200000996
0.495	Homo sapiens, Similar to RIKEN cDNA 0610030G03 gene, clone MGC:
0.489	Ras association (RalGDS/AF-6) domain family 1^RASSF1^NM_007182^
0.479	Glial cells missing homolog a (Drosophila)^GCMA^AB047819^28346^
0.423	Homo sapiens clone 24734 mRNA sequence^N/A^AF070625^12440^H2000
0.417	G protein-coupled receptor 35^GPR35^NM_005301^239891^H200015689
0.416	Homo sapiens, clone MGC:14381 IMAGE:4299817, mRNA, complete cds
0.375	KIAA0170 gene product^KIAA0170^NM_014641^277585^H200017229
0.371	KIAA0775 gene product^KIAA0775^NM_014726^94790^H200010662
0.37	Solute carrier family 20 (phosphate transporter), member 1^SLC2
0.327	Chromosome 14 open reading frame 4^C14orf4^AB058768^179260^H200
0.306	Homo sapiens mRNA; cDNA DKFZp564C142 (from clone DKFZp564C142)^
0.291	RAB3D, member RAS oncogene family^RAB3D^NM_004283^251376^H20001
0.254	Homo sapiens cDNA FLJ13691 fis, clone PLACE2000100^N/A^AK023753
0.247	Protocadherin 1 (cadherin-like 1)^PCDH1^NM_032420^79769^H200006
0.149	Hypothetical protein MGC4677^MGC4677^NM_052871^337986^H20001985
0.113	Annexin A2 pseudogene 1^ANXA2P1^M62896^348252^H200020164
0.0905	HLA-G histocompatibility antigen, class I, G^HLA-G^NM_002127^73
0.0388	Hypothetical protein FLJ23467^FLJ23467^NM_024575^16179^H2000025
0.0046	Acrosomal vesicle protein 1^ACRV1^NM_001612^169222^H200007794

We have synthesized cDNA from all the cell lines treated with either DN FGFR or GFP to use in Quantitative Real time RT-PCR analysis. Some of the interesting genes have been studied by this assay to verify their differential expression in DN FGFR treated cells. So far we have studied four genes including PCDH1, AKT3, AKT1 and ECT2. PCDH1 seemed to be interesting initially. However, after Quantitative Real time RT-PCR experiments, we did not see a consistent pattern of its expression in all DN FGFR treated cell lines. It would be more crucial for this study to find a candidate gene that plays an important role in FGFR signaling in all cell lines. Therefore, we did not proceed with this gene further.

As seen in Figure 10, the relative expression of AKT3 was significantly decreased 24 hr and 48 hr after treatment with DN FGFR in C4-2B cell line. LAPC4 cell line also showed similar pattern in earlier time points. More detail analysis of AKT3 and AKT1 in other cell lines in mRNA and protein levels is in progress. It will be significantly important if we can show that DN FGFR can disrupt the AKT pathway since this pathway is also involved in cell survival. We need more convincing data to make this conclusion and the experiments to elucidate this possibility are in progress.

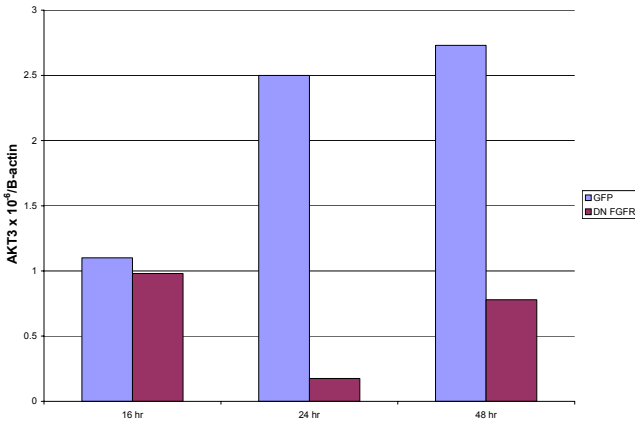

Figure 10. Relative expression of AKT3 in C4-2B cell line treated with gfp or DN FGFR.

The epithelial cell transforming gene 2 (ECT2) plays a critical role in cytokinesis and is phosphorylated in G2 and M phases of the cell cycle. It's drosophila homolog pbl has been shown to be induced by growth factors and FGF Receptor Heartless (HTL)[Schumacher et al., 2004;Saito et al., 2003]. Therefore, we thought to study this gene in our system. As shown in Figure 11, the expression of ECT2 was down-regulated in C4-2B cells in 16 and 48 hrs. We will extend this work to other cell lines as well. Additional microarray experiments and analysis are in progress to determine significant genes critical in FGFR signaling pathway.

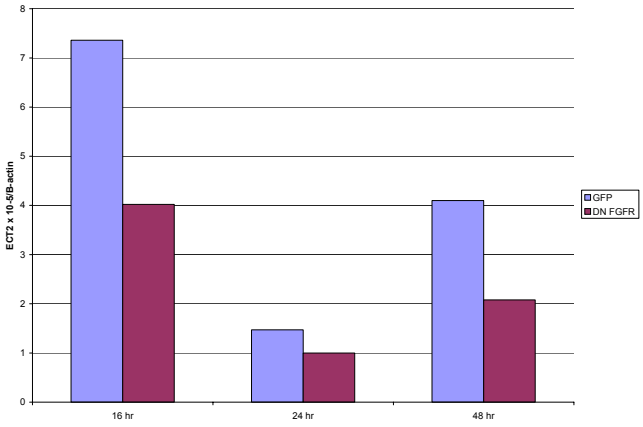

Figure 11. Relative expression of ECT2 in C4-2B cell line treated with gfp or DN FGFR.

Recently, Biosorce International, Inc., (Camarillo, CA), introduced a Mercator PhosphoArray Kit that is compatible with our Instruments. This is a protein

microarray detecting phosphorylation status of 10 proteins, including EGFR, FAK, Src, Paxillin, Akt, JNK1/2, p38, HSP27, ATF2 and CREB. These proteins are involved in different signaling pathways critical for cell migration, invasion and survival. We have done one preliminary experiment with this kit and obtained a promising data with p38 in DU145 cells treated with DN FGFR. P38 is involved in kinase activation loop and responds to stress signals. We will determine the activity of this protein in other cell lines we have. Since we already have set up the system and have the lysates, it should not take us long to complete these experiments. However, we understand that some of the data obtained from these experiments need to be verified in other systems and studied further which is beyond the scope of this project.

KEY RESEARCH ACCOMPLISHMENTS:

- Verification of DN FGFR effect on proliferation, survival and cell cycle of additional prostate cancer cell lines to determine FGF receptor signaling is essential for viability of human prostate cancer cells and disruption of this signaling via expression of a dominant negative FGF receptor-1 protein in human prostate cancer cells might contribute to the death of cancer cells *in vitro* and *in vivo*.

- The G2/M transition may be a critical checkpoint in prostate cancer.

- Identification of increased CDC25C phosphatase activity and it's biologically active spliced form in prostate cancer and the role of fibroblast growth factor receptor signaling in its activity.

REPORTABLE OUTCOMES:

Published abstracts:

Ozen M and Ittmann M: Increased CDC25C Phosphatase Activity in Prostate Cancer: Correlation to Biochemical Recurrence. The Journal of Molecular Diagnostics 2004, (6)4: 431.

Ozen M, Dixit S and Ittmann M: Molecular profiling of differentially expressed genes in response to FGFR disruption in prostate cancer. the Journal of Molecular Diagnostics 7 (5): 680, 2005.

Full Articles:

1. Ozen M and Ittmann M: Increased expression and activity of CDC25C phosphatase and an alternatively spliced variant in prostate cancer. Clinical Cancer research 11(13): 4701-6, 2005.

CONCLUSIONS:

A research in this report supports that FGF receptor signaling is essential for viability of human prostate cancer cells and disruption of this signaling via expression of a dominant negative FGF receptor-1 protein in human prostate cancer cells might contribute to the death of cancer cells. These findings reveal that prostate cancer cells treated with DN FGFR is arrested G2/M phase of cell cycle and eventually die. FGF signaling modulated *CDC25C* activity in prostate cancer, and in this manner can promote progression through the G2/M checkpoint. *CDC25C* protein is upregulated in comparison to normal prostate tissue and is present almost exclusively in its active dephosphorylated form. Expression of a biologically active alternatively spliced *CDC25C* isoform is also increased in prostate cancer. A better understanding of the mechanism by which FGF signaling is regulated and determining other molecules involved in this pathway contributing tumor growth and survival will facilitate the development of cancer therapies to target FGF signaling pathway. Our *in vivo* experiments showed that AdDN FGFR can be used as therapeutic agent in prostate cancers in nude mice. More studies need to be done to show the validity of this approach in humans.

REFERENCES:

Baldin V, Cans C, SupertiFurga G, Ducommun B (1997) Alternative splicing of the human CDC25B tyrosine phosphatase. Possible implications for growth control? *Oncogene* 14: 2485-2495

Bureik M, Rief N, Drescher R, Jungbluth A, Montenarh M, Wagner P (2000) An additional transcript of the cdc25C gene from A431 cells encodes a functional protein. *International Journal of Oncology* 17: 1251-1258

Craft N, Shostak Y, Carey M, Sawyers CL (1999) A mechanism for hormone-independent prostate cancer through modulation of androgen receptor signaling by the HER-2/neu tyrosine kinase. *Nature Medicine* 5: 280-285

Dunphy WG, Kumagai A (1991) The Cdc25 Protein Contains An Intrinsic Phosphatase-Activity. *Cell* 67: 189-196

Giri D, Ropiquet F, Ittmann M (1999) Alterations in expression of basic fibroblast growth factor (FGF) 2 and its receptor FGFR-1 in human prostate cancer. *Clinical Cancer Research* 5: 1063-1071

Graves PR, Lovly CM, Uy GL, Piwnica-Worms H (2001) Localization of human Cdc25C is regulated both by nuclear export and 14-3-3 protein binding. *Oncogene* 20: 1839-1851

Graves PR, Yu LJ, Schwarz JK, Gales J, Sausville EA, O'Connor PM, Piwnica-Worms H (2000) The Chk1 protein kinase and the Cdc25C regulatory pathways are targets of the anticancer agent UCN-01. *Journal of Biological Chemistry* 275: 5600-5605

Green AP, Huang JJ, Scott MO, Kierstead TD, Beaupre I, Gao GP, Wilson JM (2002) A new scalable method for the purification of recombinant adenovirus vectors. *Human Gene Therapy* 13: 1921-1934

Hoffmann I (2000) The role of Cdc25 phosphatases in cell cycle checkpoints. *Protoplasma* 211: 8-11

Izumi T, Maller JL (1995) Phosphorylation and Activation of the Xenopus Cdc25 Phosphatase in the Absence of Cdc2 and Cdk2 Kinase-Activity. *Molecular Biology of the Cell* 6: 215-226

Navone NM, Olive M, Ozen M, Davis R, Troncoso P, Tu SM, Johnston D, Pollack A, Pathak S, von Eschenbach AC, Logothetis CJ (1997) Establishment of two human prostate cancer cell lines derived from a single bone metastasis. *Clinical Cancer Research* 3: 2493-2500

Olmsted-Davis EA, Gugala Z, Gannon FH, Yotnda P, McAlhany RE, Lindsey RW, Davis AR (2002a) Use of a chimeric adenovirus vector enhances BMP2 production and bone formation. *Human Gene Therapy* 13: 1337-1347

Olmsted-Davis EA, Gugala Z, Gannon FH, Yotnda P, McAlhany RE, Lindsey RW, Davis AR (2002b) Use of a chimeric adenovirus vector enhances BMP2 production and bone formation. *Human Gene Therapy* 13: 1337-1347

Ozen M, Giri D, Ropiquet F, Mansukhani A, Ittmann M (2001) Role of fibroblast growth factor receptor signaling in prostate cancer cell survival. *Journal of the National Cancer Institute* 93: 1783-1790

Peng CY, Graves PR, Thoma RS, Wu ZQ, Shaw AS, PiwnicaWorms H (1997) Mitotic and G(2) checkpoint control: Regulation of 14-3-3 protein binding by phosphorylation of Cdc25C on serine-216. *Science* 277: 1501-1505

Polnaszek N, Kwabi-Addo B, Peterson LE, Ozen M, Greenberg NM, Ortega S, Basilico C, Ittmann M (2003) Fibroblast growth factor 2 promotes tumor progression in an autochthonous mouse model of prostate cancer. *Cancer Research* 63: 5754-5760

Saito S, Tatsumoto T, Lorenzi MV, Chedid M, Kapoor V, Sakata H, Rubin J, Miki T (2003) Rho exchange factor ECT2 is induced by growth factors and regulates cytokinesis through the N-terminal cell cycle regulator-related domains. *J Cell Biochem* 90: 819-836

Schumacher S, Gryzik T, Tannebaum S, Muller HA (2004) The RhoGEF Pebble is required for cell shape changes during cell migration triggered by the Drosophila FGF receptor Heartless. *Development* 131: 2631-2640

Shayakhmetov DM, Papayannopoulou T, Stamatoyannopoulos G, Lieber A (2000) Efficient gene transfer into human CD34(+) cells by a retargeted adenovirus vector. *Journal of Virology* 74: 2567-2583

Sramkoski RM, Pretlow TG, Giaconia JM, Pretlow TP, Schwartz S, Sy MS, Marengo SR, Rhim JS, Zhang DS, Jacobberger JW (1999) A new human prostate carcinoma cell line, 22R upsilon 1. *In Vitro Cellular & Developmental Biology-Animal* 35: 403-409

Strausfeld U, Labbe JC, Fesquet D, Cavadore JC, Picard A, Sadhu K, Russell P, Doree M (1991) Dephosphorylation and Activation of A P34Cdc2 Cyclin-B Complex Invitro by Human Cdc25 Protein. *Nature* 351: 242-245

Takahashi, H. Studies on the expression of fibroblast growth factors and fibroblast growth factor receptors in human prostate cancer. Nippon Hinyokika Gakkai Zasshi 89, 836-845. 1998.

Thalmann GN, Sikes RA, Wu TT, Degeorges A, Chang SM, Ozen M, Pathak S, Chung LW (2000) LNCaP progression model of human prostate cancer: androgen-independence and osseous metastasis. *Prostate* 44: 91-103

Turowski P, Franckhauser C, Morris MC, Vaglio P, Fernandez A, Lamb NJC (2003) Functional cdc25C dual-specificity phosphatase is required for S-phase entry in human cells. *Molecular Biology of the Cell* 14: 2984-2998

Tuxhorn JA, McAlhany SJ, Yang F, Dang TD, Rowley DR (2002) Inhibition of transforming growth factor-beta activity decreases angiogenesis in a human prostate cancer-reactive stroma xenograft model. *Cancer Res* 62: 6021-6025

Wegener S, Hampe W, Herrmann D, Schaller HC (2000) Alternative splicing in the regulatory region of the human phosphatases CDC25A and CDC25C. *European Journal of Cell Biology* 79: 810-815

Yotnda P, Onishi H, Heslop HE, Chen D, Chiu W, Piedra PA, Takahashi S, Barry M, Davis A, Templeton NS, Brenner MK (2002) Targeting adenovectors to hemopoietic cells. *Blood Cells Molecules and Diseases* 28: 347

Yotnda P, Onishi H, Heslop HE, Shayakhmetov D, Lieber A, Brenner M, Davis A (2001) Efficient infection of primitive hematopoietic stem cells by modified adenovirus. *Gene Therapy* 8: 930-937

Zeng Y, Forbes KC, Wu ZQ, Moreno S, Piwnica-Worms H, Enoch T (1998) Replication checkpoint requires phosphorylation of the phosphatase Cdc25 by Cds1 or Chk1. *Nature* 395: 507-510

APPENDICES:

A manuscript by Ozen M and Ittmann M: Increased CDC25C phosphatase activity in prostate cancer: role of fibroblast growth factor receptor signaling. Clinical Cancer Research (in press).

Acceptance letter for the above manuscript

An abstract published in the Journal of Molecular Diagnostics.

Increased Expression and Activity of CDC25C Phosphatase and an Alternatively Spliced Variant in Prostate Cancer

Mustafa Ozen and Michael Ittmann

Abstract Alterations in the control of cell cycle progression have been implicated in a wide variety of malignant neoplasms, including prostate cancer. CDC25 phosphatases belong to the tyrosine phosphatase family and play a critical role in regulating cell cycle progression by dephosphorylating cyclin-dependent kinases at inhibitory residues. CDC25C plays an important role in the G_2-M transition by activating Cdc2/Cyclin B1 complexes. To determine whether CDC25C activity is altered in prostate cancer, we have examined the expression of CDC25C and an alternatively spliced variant in human prostate cancer samples and cell lines. CDC25C protein is up-regulated in prostate cancer in comparison with normal prostate tissue and is present almost exclusively in its active dephosphorylated form. Expression of a biologically active alternatively spliced CDC25C isoform is also increased in prostate cancer and expression of alternatively spliced CDC25C is correlated to occurrence of biochemical (prostate-specific antigen) recurrence. We have also developed a quantitative reverse transcriptase-PCR analysis of Ki-67 expression as a method of measuring proliferative activity in prostate cancer from RNA samples. Based on this analysis of Ki67 expression, some but not all of this increase in CDC25C and its alternatively spliced variants is correlated with increased proliferation in prostate cancer. This data suggests that CDC25C might play an important role in prostate cancer progression and could be used to monitor and predict the aggressiveness of this disease.

Abnormal expression and/or activity of cell cycle regulatory proteins have been identified in a wide variety of malignant neoplasms, including prostate cancer. Cell cycle progression is controlled by the sequential activities of cyclin-dependent kinases, whose activities are tightly regulated by cyclins, cyclin-dependent kinase inhibitors, and a variety of other proteins. Several groups have shown increased expression of cyclin B1, which plays a critical role in the G_2-M transition, in human prostate cancers (1, 2). Recent work by Maddison et al. (3) has shown increased levels of cyclin B1 in poorly differentiated and androgen-independent prostate cancers in the TRAMP mouse model of prostate cancer. During G_2, the Cdc2/Cyclin B complex is kept inactive by phosphorylation of Cdc2 by Wee1. At the onset of mitosis, Cdc2/Cyclin B complexes are dephosphorylated by CDC25 phosphatase leading to increased kinase activity (4–6). Our laboratory has shown previously that disruption of fibroblast growth factor signaling in prostate cancer cells leads to decrease in Cdc2 kinase activity and arrest in G_2 followed by cell death (7). These findings imply that the G_2-M transition may be a critical checkpoint in prostate cancer.

CDC25 phosphatases belong to the tyrosine phosphatase family and play a critical role in regulating cell cycle progression by dephosphorylating cyclin-dependent kinases at inhibitory residues. In human cells, CDC25 proteins are encoded by a multigene family, consisting of *CDC25A*, *CDC25B*, and *CDC25C* (8). In late G_2, CDC25C dephosphorylates Cdc2 on both Thr^{14} and Tyr^{15}, leading to the activation of Cdc2/Cyclin B complexes (9–11) and progression through the G_2-M checkpoint. Phosphorylation of Ser^{216} of CDC25C throughout interphase and upon G_2 checkpoint activation has been found to negatively regulate the activity of CDC25C by cytoplasmic sequestration (12, 13) and a positive feedback loop has been proposed between Cdc2 and CDC25C (11, 13–15). Activated Chk kinases can phosphorylate CDC25C at Ser^{216}, blocking the activation of Cdc2 and transition into the M phase (16). Another aspect of CDC25 regulation is alternative splicing that may produce at least five CDC25B variants (17), and splice variants are also reported for CDC25A and CDC25C (18, 19). The activity and regulation of CDC25C in prostate carcinoma has not been previously examined, despite its potentially important role in the G_2-M transition in this common malignancy.

To determine whether CDC25C plays a role in prostate cancer, we have examined the expression of CDC25C and an alternatively spliced variant in human prostate cancer samples

Authors' Affiliations: Department of Pathology, Baylor College of Medicine and Michael E. DeBakey, Department of Veterans Affairs Medical Center, Houston, Texas
Received 12/10/04; revised 3/18/05; accepted 4/1/05.
Grant support: Department of Defense Prostate Cancer Research Program grant DAMD17-03-1-0006 (M. Ozen), Department of Veterans Affairs Merit Review funding (M. Ittmann), National Cancer Institute grant P50CA058204 (Baylor prostate cancer Specialized Programs of Research Excellence program), and Moran Foundation award.
The costs of publication of this article were defrayed in part by the payment of page charges. This article must therefore be hereby marked *advertisement* in accordance with 18 U.S.C. Section 1734 solely to indicate this fact.
Requests for reprints: Michael Ittmann, Research Service, Michael E. DeBakey Veterans Affairs Medical Center, 2002 Holcombe Boulevard, Houston, TX 77030. Phone: 713-791-1414, ext. 4008; Fax: 713-794-7938; E-mail: mittmann@bcm.tmc.edu.

and cell lines at both the protein and RNA levels. CDC25C protein is up-regulated in comparison with normal prostate tissue and is present predominantly in its active dephosphorylated form. At the transcriptional level, CDC25C and an alternatively spliced variants were both overexpressed in prostate cancer. The expression of the spliced variants were correlated with biochemical recurrence.

Materials and Methods

Tissue acquisition and extraction. Normal peripheral zone, hyperplastic transition zone (benign prostatic hyperplasia), and cancer tissues were collected from men undergoing radical prostatectomy for clinically localized prostate cancer by Baylor prostate cancer Specialized Programs of Research Excellence Tissue Core and snap frozen. Benign tissues were confirmed to be free of cancer and cancer tissues contained at least 70% carcinoma. RNAs were extracted from 17 normal peripheral zone tissues, seven benign prostatic hyperplasia tissues, and 58 prostate cancers using TRIzoL Reagent (Invitrogen, Carlsbad, CA) as described in the manufacturer's protocol. We analyzed 20 cancers with no evidence of prostate-specific antigen (PSA) recurrence after 5 years of follow-up, 19 cancers with delayed PSA recurrence (mean time to recurrence of 34.1 months), and 19 cancers with early recurrence (i.e., <1 year; mean time to recurrence of 4.5 months). PSA recurrence was defined as serum PSA of >0.2 ng/mL. Protein extracts were prepared as described previously (20) from 10 cancers and eight normal peripheral zone tissues.

Reverse transcriptase-PCR and agarose gel electrophoresis. RNAs extracted from the prostate tissues were first reverse transcribed as previously described (21) and analyzed for the presence of two different cDNAs for CDC25C using the following primers flanking the deletions of the CDC25C sequence: forward, 5′-AGAGAGAAGCTTATGTCTACGGAACTCTTCTCATCC-3′; reverse, 5′-CCCAAATATTTCATTTCACTGTCC-3′ as described previously by Bureik et al. (19). The β-actin primers were as described previously (22). Thirty-five cycles with the following program were done: denaturation at 94°C for 1 minute, annealing at 60°C for 1.5 minutes, elongation at 72°C for 1 minute followed by 5 minutes extension at 72°C. The reaction was done with the Takara kit (Takara Mirus, Madison, WI) following the manufacturer's protocol. The PCR products were analyzed on a 1.5% agarose gels and stained with ethidium bromide.

Cell lines. DU145, PC3, and LNCaP human prostate cancer cell lines were cultured in RPMI 1640 supplemented with 1% antibiotic and antimycotic (Invitrogen Life Technologies, Carlsbad, CA) and 10% fetal bovine serum.

Quantitative real-time PCR and primer design. Real-time reverse transcriptase-PCR (RT-PCR) was carried out in iCycler real-time thermal cycler (Bio-Rad, Hercules, CA) as described previously (22), incorporating the optimized PCR reaction conditions for each primer set. Oligonucleotide primers for CDC25C were carefully designed to cross exon/intron regions and to avoid self-complementarity or the formation of primer-dimers and hairpins. Two primer sets, one detecting only the full length CDC25C by binding in the region deleted in the alternatively spliced variant (forward, 5′-GCCACTCAGCTTACCACTTC-3′; reverse, 5′-ATTTCATTTCACTGTCCACCAAG-3′) and the other detecting both spliced variant and the full-length CDC25C (forward, 5′-GACACCCAGAAGAGAATAATCATC-3′; reverse, 5′-CGACACCTCAGCAACTCAG-3′) were used. Alternatively spliced transcript levels were calculated by subtraction of full-length CDC25C transcript levels from the total CDC25C levels. This approach allows quantitation of the major alternatively spliced isoforms detected in prostate cancer cells, specifically the C5 and C4 variants described by Wegener et al. (18). The primers for Ki67 were as follows: forward, 5′-ACGAGACGCCTGGTTACTA TC-3′; reverse, 5′-GCTCATCAATAACAGACC CATTTAC-3′. The β-actin primers were as described previously (22). The threshold cycle (C_t) values in log linear range representing the detection threshold values was used for quantitation and expressed as copy numbers based on a standard curve generated using plasmid DNA.

Western blot analysis. The tissue samples were homogenized and lysed in lysis buffer (20) and cleared by centrifugation for 10 minutes in a microcentrifuge at 4°C. Protein concentration was determined using a Bio-Rad protein assay. The lysates were then boiled in sample buffer, centrifuged, and 30 μg of supernatant protein subjected to SDS-PAGE electrophoresis using a 10% gel. The resolved proteins were electrotransferred to nitrocellulose membranes and then blocked with PBS with 0.5% Tween 20 (PBST) containing 5% fat-free milk. Western blot for CDC25C was done using 500 ng/mL of polyclonal anti-CDC25C antibody (C20, Santa Cruz Biotechnology, Santa Cruz, CA) and anti-phosphoCDC25C (Ser^{216}) antibody (901, Cell Signaling Technology, Beverly, MA) at 4°C for 16 hours. The membranes were then washed with PBST and treated with appropriate secondary antibody. The antigen-antibody reaction was visualized using an enhanced chemiluminescence assay (Amersham, Arlington Heights, IL) and exposure to enhanced chemiluminescence film (Amersham). Control antibody was an anti-β-actin monoclonal antibody (A5316, Sigma, St. Louis, MO) used at a 1:5,000 dilution. To determine the specificity of the bands observed in Western blots for CDC25, anti-CDC25C antibody was preincubated with 5-fold molar excess of the blocking peptide (sc-327 P, Santa Cruz Biotechnology) for 2 hours at room temperature before use in the Western blot protocol. For quantitative Western blotting studies, the intensities of the bands on the Western blots were quantified as densitometric units by using the GelExpert software package supplied with the Nucleovision gel imaging system (Nucleo Tech Corp., Hayward, CA).

Results

Activity of CDC25C protein in clinically localized human prostate cancers. To evaluate the *in vivo* activity of CDC25C in prostate cancer tissues, we determined the levels of total and phosphorylated CDC25C protein in the lysates from normal prostate peripheral zone and prostate cancer tissue samples. Out of nine evaluable cancer samples, only two had readily detectable amounts of phospho-CDC25C (Fig. 1). In contrast, in the same blots normal prostate peripheral zone samples had detectable phospho-CDC25C protein in six of eight samples. Total CDC25C protein was detectable in six of nine cancer cases, whereas only two of eight normal tissue samples showed detectable total CDC25C when analyzed in the same blots (Fig. 1). Thus, in cancer tissues there is both markedly increased CDC25C protein and much less of its inactive phosphorylated form.

Alternatively spliced CDC25C variant is detected in prostate cancer RNA and in prostate cancer cell lines. In addition to the full-length CDC25C protein examined above, there are alternatively spliced of CDC25C transcripts that have been detected in a number of cancer cell lines (18, 19). The immunoglobulin heavy chain that is present in large amounts in some patient samples may interfere with direct measurement of the alternatively spliced proteins in clinical samples. We therefore analyzed RNAs from prostate cancer cell lines and a second set of clinically localized prostate cancers for the presence of the CDC25C alternatively spliced variants using RT-PCR and electrophoresis on agarose gels (Fig. 2A). The full-length wild-type (WT) and alternatively spliced CDC25C transcripts are present in both LNCaP and DU145 prostate cancer cell lines (Fig. 2A). The major alternatively spliced isoform corresponds to the C5 variant described by Wegener

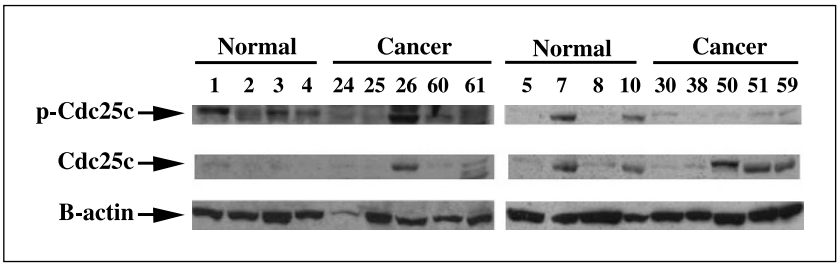

Fig. 1. CDC25C protein levels in clinically localized human prostate cancers. Normal peripheral zone and cancer tissues were collected from men undergoing radical prostatectomy for clinically localized prostate cancer by Baylor prostate cancer Specialized Programs of Research Excellence Tissue Core and snap frozen. Protein lysates were prepared as described in Materials and Methods. Western blot for CDC25C was done using polyclonal anti-CDC25C antibody or a Ser^{216} phosphorylation site specific antibody. An anti-β-actin monoclonal antibody was used as loading control. The numbers representing samples are obtained from our clinical database. Sample 24 was not included in the analysis due to low β-actin signal, indicating inadequate protein in this lane.

et al. (18). Other variant transcripts, intermediate in size between the WT and C5 transcripts were present in lower amounts as well. The C5 CDC25C transcript was detectable by this methodology in 29 of 58 prostate cancer RNAs. In contrast, only 3 of 17 normal peripheral zone samples and none of the seven benign prostatic hyperplasia samples had detectable quantities of this variant. The difference between the cancer and benign samples was statistically significant (P = 0.002, Fisher exact test). In addition, the presence of the variant was strongly associated with the occurrence of biochemical (PSA) recurrence. Overall, the variant was present in cancer samples from 23 of 38 patients with biochemical recurrence but only 6 of 20 without PSA recurrence. This difference was statistically significant (P = 0.027, Pearson's χ^2). Since PSA recurrence, particularly early PSA recurrence, is associated with aggressive disease and decreased patient survival, this observation implies

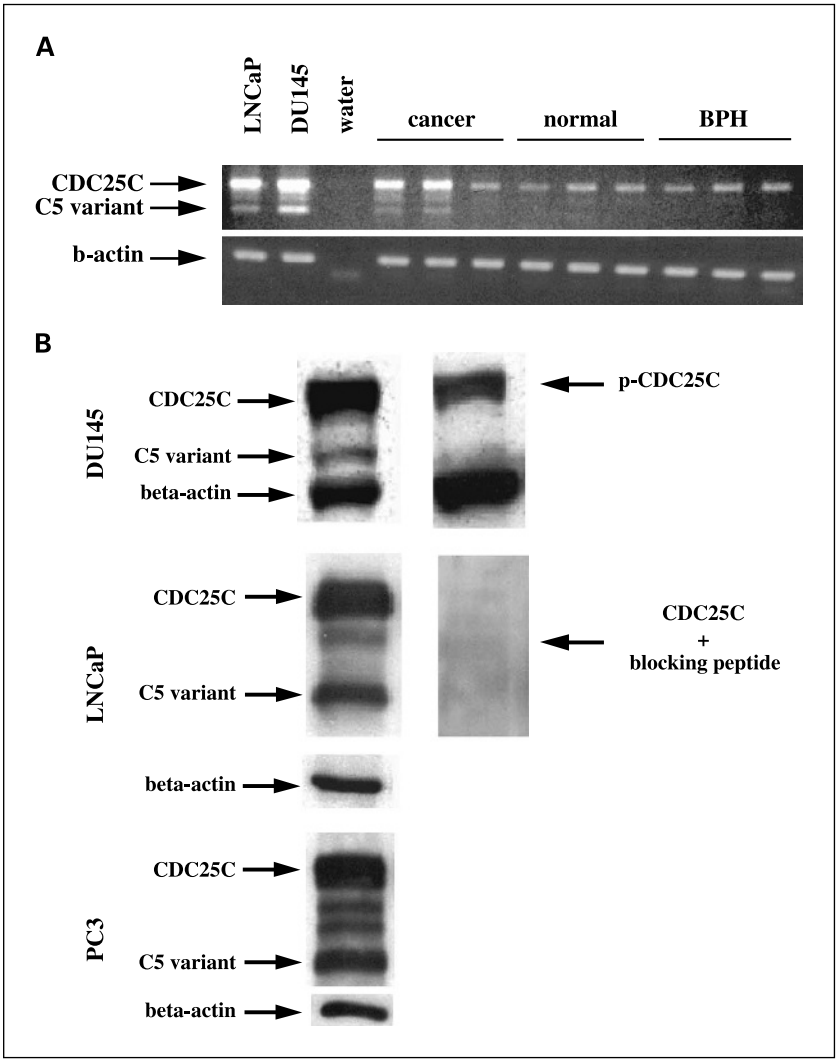

Fig. 2. Expression of full-length and alternatively spliced CDC25C mRNA and/or proteins in prostate tissues and prostate cancer cell lines. *A*, RNAs were extracted from normal peripheral zone tissues, benign prostatic hyperplasia (*BPH*) tissues, and prostate cancer tissue samples using TRIzoL Reagent as described by the manufacturer's protocol and analyzed by RT-PCR as described in Materials and Methods. Bands corresponding to the full-length (512 bp) and variant mRNA (293 bp). Three samples each of cancer, normal, and benign prostatic hyperplasia groups. RT-PCR with β-actin primers was used as a control for cDNA quantity. *B*, protein lysates from prostate cancer cell lines are subjected to Western blot analysis using the appropriate antibodies as described in Materials and Methods. Preincubation with peptide immunogen for the CDC25C antibody was used to determine the specificity of the two CDC25C bands.

that expression of the variant mRNA is higher in aggressive prostate cancers. No statistically significant correlation of expression of the CDC25C variant with preoperative PSA or pathologic stage was detected. As illustrated in Fig. 2A, the cancer tissues also seemed to express increased amounts of WT mRNA in addition to expressing the variant mRNA, consistent with our observation of increased levels of WT CDC25C protein in the prostate cancer extracts.

We studied the presence of alternatively spliced CDC25C variant protein in prostate cancer cell lines to confirm its expression at the protein level (Fig. 2B). Both the WT and C5 variant are expressed in all three of the commonly used prostate cancer cell lines (DU145, LNCaP, and PC3). The specificity of the antibody for the WT and C5 variant was confirmed by preincubation of the anti-CDC25C antibody with excess peptide immunogen, which abolished both bands in a Western blot of LNCaP cell extract.

Other variant CDC25C proteins are also present in lower amounts, particularly in PC3 cells. To determine if the C5 variant is phosphorylated at the Ser^{216} residue, which is associated with cytoplasmic sequestration and loss of biological activity, we analyzed Western blots of DU145 protein extracts with a Ser^{216}-specific anti-phospho-CDC25C antibody. No phosphorylation at Ser^{216} was detected in the C5 variant despite the readily detectable phosphorylation of the WT protein.

To assess the relationship between the level of WT and spliced variant proteins and mRNA levels, we carried out quantitative RT-PCR to detect WT or spliced variant mRNAs and did Western blots with serial dilutions of protein extracts from the same cells with anti-CDC25C antibody. We used both actively proliferating and confluent DU145 cells in these studies. As described in Materials and Methods, the quantitative RT-PCR assay used measures both the C4 and C5 mRNA variants (and potentially other variants) as alternatively spliced transcripts, although based on the gel electrophoresis in Fig. 2A, the C5 variant seems the dominant form. Western blots were scanned to quantitatively determine the band intensity of WT and alternatively spliced isoforms and the ratio of protein band intensity (as densitometric units) per μg protein to RNA copy number determined. For actively growing cells, this ratio was 11.1×10^{-3} for WT versus 2.21×10^{-3} for the spliced variant and for confluent cells this ratio was 2.8×10^{-3} for WT versus 0.94×10^{-3}. Thus, the WT transcript is associated with approximately three to five times more protein per transcript when compared with the alternative spliced transcript. Whether this is due to differences in translation efficiency or protein stability (or both) is not known.

To confirm our qualitative observations in the clinical samples with more rigorous quantitative data, we determined the expression levels of CDC25C WT and the spliced variants by real-time RT-PCR assay. Quantitative analysis of expression of WT CDC25C mRNA revealed a 4-fold increase in WT mRNA in cancer tissues relative to normal tissues (0.3 ± 0.08 CDC25C transcripts/10^4 β-actin transcripts in normal versus 1.28 ± 0.2 CDC25C transcripts/10^4 β-actin transcripts in cancer tissues; mean ± SE). This difference was statistically significant ($P < 0.001$, Mann-Whitney rank sum test). In addition, as can be seen in Fig. 3, there is a statistically significant increase in the expression of both total CDC25C and CDC25C splice variant mRNA in recurrent prostate cancers ($P = 0.037$ and $P < 0.001$, respectively, Mann-Whitney) when compared with nonrecurrent cancers. This increase is particularly marked in the prostate cancers with early recurrence. It should be noted that although the amount of spliced variant mRNAs in the recurrent cancers is about equal to the amount of WT mRNA, the amount of spliced variant protein(s) is probably 3- to 5-fold lower, based on the quantitative studies in DU145 cells described above.

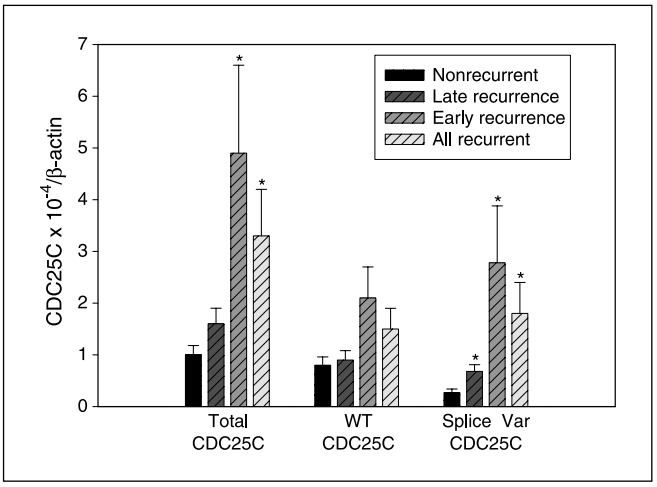

Fig. 3. Correlation of PSA recurrence with expression of CDC25C mRNAs relative to β-actin as determined by real-time RT-PCR. Total and WT mRNA transcript levels were determined by quantitative RT-PCR as described in Materials and Methods. Alternatively spliced transcript levels were calculated by subtraction of WT CDC25C transcript levels from the total CDC25C levels. *Columns*, means; *bars*, ±SE. *, statistically significant differences.

Determination of Ki-67 RNA levels by real-time quantitative reverse transcriptase-PCR as measurement for proliferative activity and normalization of CDC25C levels. Because CDC25 is involved in control of exit from the G_2 phase of the cell cycle, it is likely that the differences between normal and cancer tissues and nonrecurrent and recurrent cancer tissues may be associated with differences in proliferative activity. To address this question, we designed a real-time RT-PCR assay to determine RNA levels of the proliferation marker, Ki-67. The monoclonal antibody recognizing Ki-67 is routinely used in oncology to assess the proliferative index of tumor cells. Ki-67 transcript levels were ~2-fold higher in the cancer tissues when compared with normal peripheral zone tissues ($P = 0.001$, Mann-Whitney). As seen in Fig. 4, relative expression of Ki-67 to β-actin was increased in Gleason score 7 to 9 cases (versus Gleason scores 5-6) and in cases with extracapsular extension and seminal vesicle invasion (versus organ-confined cancers), although not in cases with lymph node metastasis (Fig. 4). Ki-67 mRNA was also increased in prostate cancers that recurred (versus nonrecurrent cancers), particularly the cancers with early PSA recurrence (Fig. 4). The difference between the Ki-67 transcript levels in nonrecurrent versus those with early recurrence was statistically significant ($P = 0.032$, Mann-Whitney). Overall, as expected, increased Ki-67 transcript levels were associated with pathologic and clinical variables indicative of aggressive disease.

We then examined the correlation between CDC25C and Ki-67 transcript levels using the Pearson Product Moment test. There was a statistically significant correlation between the Ki-67 transcript levels and total, WT and variant CDC25C transcript levels ($P < 0.001$, $P < 0.001$, $P < 0.018$, respectively).

The correlation coefficients ranged from 0.5 to 0.6, implying that a substantial fraction, but not all, of the variance in CDC25C levels is associated with differences in proliferation. As an alternative way to examine this association, we normalized expression of CDC25C expression levels using Ki-67 transcript levels determined on the same cDNAs rather than β-actin levels (Fig. 5). Using this normalization, expression levels of the CDC25C splice variants was still significantly increased in patients with subsequent biochemical recurrence, including patients with either early (P = 0.041) and late recurrence (P = 0.044). The level of the Ki-67 normalized alternatively spliced CDC25c mRNA was also significantly higher in cancers with higher Gleason score (Gleason 7-9 versus 5-6; P = 0.044, Mann-Whitney) and was higher in cases with extracapsular extension, seminal vesicle invasion, and lymph node metastasis, although these differences were not statistically significant.

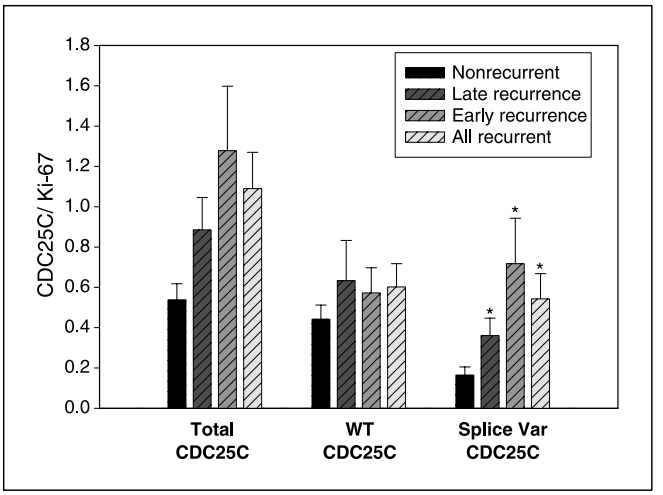

Fig. 5. Relative expression of CDC25C to Ki67 in prostate cancer. Total and WT mRNA transcript levels were determined by quantitative RT-PCR as described in Materials and Methods. Alternatively spliced transcript levels were calculated by subtraction of WT CDC25C transcript levels from the total CDC25C levels. Samples are grouped by their recurrence status and interval. *, statistically significant differences in each group.

Discussion

CDC25A and CDC25B have been shown to collaborate with either mutation in the RAS oncogene or loss of retinoblastoma protein in transformation and, in this initial report, CDC25B protein was increased in 32% of human breast cancers (23). Subsequently, increased expression of CDC25A has been shown in head and neck (24), non–small cell lung (25), gastric (26), and colon cancers (27), whereas CDC25B is increased in non-Hodgkin's lymphomas (28), as well as head and neck (24), non–small cell lung (25), gastric (26), colon (27), pancreatic (28), and prostate cancers (29). In contrast, increased expression of CDC25C has only been reported in a fraction of colon (27) and endometrial cancers (30). We have shown that the majority of prostate cancers have both increased total WT CDC25C protein and less phosphorylated CDC25C when compared with normal prostatic tissue. The level of WT CDC25C mRNA was increased 4-fold in cancer tissues consistent with these increased protein levels. Thus, there are significantly higher levels of WT CDC25C protein in prostate cancer and much less of its inactive phosphorylated form, consistent with a marked increase in CDC25C phosphatase activity in prostate cancer.

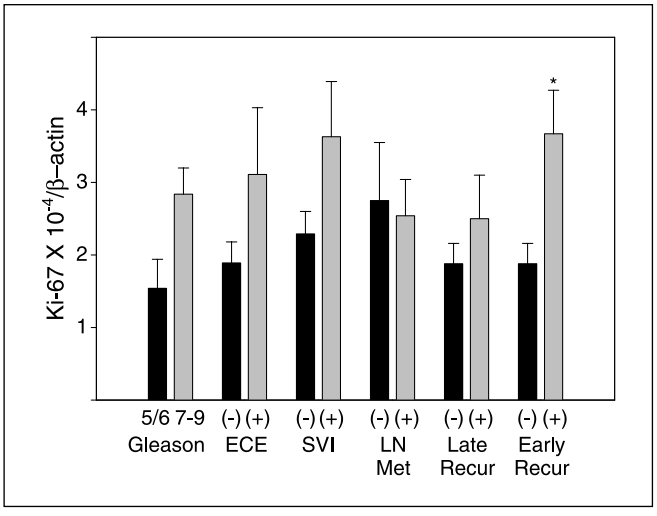

Fig. 4. Correlation of expression of Ki-67 mRNA relative to β-actin with clinical and pathologic variables in clinically localized prostate cancer. Clinical samples are grouped by Gleason grade, presence of extracapsular extension (*ECE*), seminal vesicle invasion (*SVI*), and lymph node metastasis (*LN Met*). Cases with PSA recurrence were compared with those without recurrence (−). *, statistically significant differences.

In addition to the full-length CDC25C mRNA, we detected a major alternatively spliced CDC25C in both human prostate cancers *in vivo* and in prostate cancer cell lines. This alternatively spliced transcript has a deletion of exons 3, 5, and 6 of the *CDC25C* gene and encodes a smaller protein containing the COOH-terminal catalytic domain and 17 unique amino acids. This alternatively spliced variant can complement a *CDC25C* mutant strain of *Schizosaccharomyces pombe* (19). It is interesting to note that this variant leads to an increased uncoupling of the onset of mitosis and the completion of DNA synthesis in this mutant strain of *S. pombe*, implying poor regulation of the activity of this variant protein. This alternatively spliced RNA was detected as visible band in one half of the prostate cancers analyzed but in only 16% of the benign tissues. The presence of this variant was significantly correlated with biochemical (PSA) recurrence following radical prostatectomy. Quantitative RT-PCR studies confirmed a significant increase in variant CDC25C mRNAs in prostate cancer and its correlation with PSA recurrence, particularly early PSA recurrence that is associated with aggressive disease and worse patient outcome (31). It should be noted that the quantitative RT-PCR assay detects other splice variants, particularly the C4 variant, which may also contribute to the observed correlation, although the C5 variant was the most highly expressed form. Although the spliced variant mRNA are only a portion of total CDC25C mRNA *in vivo*, it may have significant biological effects that lead to more aggressive diseases, perhaps through poor regulation of its activity. Thus, prostate cancer is characterized by multiple alterations in CDC25C that can increase its activity *in vivo*.

Based on comparison of CDC25C and Ki-67 transcript levels, there was a significant correlation of WT and variant CDC25C

transcript levels with Ki-67 transcript levels. Increased expression of CDC25C would be expected to promote progression through the G_2-M checkpoint and, particularly if associated with loss of other cell cycle checkpoint controls, would increase cellular proliferation. Further mechanistic studies to determine the basis of the increased CDC25C transcript levels in cancer may reveal whether this is a primary event associated with malignant transformation or a secondary event related other alterations in prostate cancer cells such as increased growth factor signaling.

The finding that the level of alternatively spliced CDC25C transcripts is correlated with recurrence, even after correction for proliferation by normalization to Ki67 levels indicates that expression of variant CDC25C has independent correlation with biochemical recurrence. Bureik et al. (19) have shown that expression of the major alternatively spliced CDC25C variant in *S. pombe* resulted in uncoupling of mitosis from completion of the S phase. Of note is the finding that the C5 variant does not seem phosphorylated at the inhibitory Ser^{216} residue. This site is phosphorylated by Chk kinase, which plays an important role in protecting the genomic integrity of cells following DNA damage (32). Thus, expression of the C5 variant of CDC25C could potentially result in genomic instability, which could facilitate emergence of aggressive disease. Further studies are needed to test this possibility.

In summary, we have described, for the first time, the increased activity of CDC25C phosphatase and overexpression of an alternatively spliced CDC25C mRNA in prostate cancer. Increased expression of the both total CDC25C mRNA and its spliced variant are correlated with biochemical recurrence, particularly early recurrence. Further studies need to be done to determine the role of CDC25C and its spliced variants in prostate cancer pathogenesis.

Acknowledgments

We thank the Michael E. DeBakey Veterans Affairs Medical Center for the use of their facilities.

References

1. Mashal RD, Lester S, Corless C, et al. Expression of cell cycle-regulated proteins in prostate cancer. Cancer Res 1996;56:4159–63.
2. Kallakury BV, Sheehan CE, Ambros RA, et al. Correlation of p34(cdc2) cyclin-dependent kinase overexpression, CD44s downregulation, and HER-2/*neu* oncogene amplification with recurrence in prostatic adenocarcinomas. J Clin Oncol 1998;16:1302–9.
3. Maddison LA, Huss WJ, Barrios RM, Greenberg NM. Differential expression of cell cycle regulatory molecules and evidence for a "cyclin switch" during progression of prostate cancer. Prostate 2004;58:335–44.
4. Booher RN, Holman PS, Fattaey A. Human Myt1 is a cell cycle-regulated kinase that inhibits Cdc2 but not Cdk2 activity. J Biol Chem 1997;272:22300–6.
5. Draetta G, Eckstein J. Cdc25 protein phosphatases in cell proliferation. Biochim Biophys Acta-Reviews on Cancer 1997;1332:M53–63.
6. Taylor WR, Stark GR. Regulation of the G_2/M transition by p53. Oncogene 2001;20:1803–15.
7. Ozen M, Giri D, Ropiquet F, Mansukhani A, Ittmann M. Role of fibroblast growth factor receptor signaling in prostate cancer cell survival. J Natl Cancer Inst 2001; 93:1783–90.
8. Turowski P, Franckhauser C, Morris MC, Vaglio P, Fernandez A, Lamb NJC. Functional cdc25C dual-specificity phosphatase is required for S-phase entry in human cells. Mol Biol Cell 2003;14:2984–98.
9. Graves PR, Lovly CM, Uy GL. Piwnica-Worms H, Localization of human Cdc25C is regulated both by nuclear export and 14-3-3 protein binding. Oncogene 2001;20:1839–51.
10. Dunphy WG, Kumagai A. The Cdc25 protein contains an intrinsic phosphatase-activity. Cell 1991; 67:189–96.
11. Strausfeld U, Labbe JC, Fesquet D, et al. Dephosphorylation and activation of a P34Cdc2 Cyclin-B complex *in vitro* by human Cdc25 protein. Nature 1991;351:242–5.
12. Graves PR, Yu LJ, Schwarz JK, et al. The Chk1 protein kinase and the Cdc25C regulatory pathways are targets of the anticancer agent UCN-01. J Biol Chem 2000;275:5600–5.
13. Peng CY, Graves PR, Thoma RS, Wu ZQ, Shaw AS, Piwnica-Worms H. Mitotic and G(2) checkpoint control: regulation of 14-3-3 protein binding by phosphorylation of Cdc25C on serine-216. Science 1997;277: 1501–5.
14. Hoffmann I. The role of Cdc25 phosphatases in cell cycle checkpoints. Protoplasma 2000;211:8–11.
15. Izumi T, Maller JL. Phosphorylation and activation of the *Xenopus* Cdc25 phosphatase in the absence of Cdc2 and Cdk2 kinase-activity. Mol Biol Cell 1995; 6:215–26.
16. Zeng Y, Forbes KC, Wu ZQ, Moreno S, Piwnica-Worms H, Enoch T. Replication checkpoint requires phosphorylation of the phosphatase Cdc25 by Cds1 or Chk1. Nature 1998;395:507–10.
17. Baldin V, Cans C, SupertiFurga G, Ducommun B. Alternative splicing of the human CDC25B tyrosine phosphatase. Possible implications for growth control? Oncogene 1997;14:2485–95.
18. Wegener S, Hampe W, Herrmann D, Schaller HC. Alternative splicing in the regulatory region of the human phosphatases CDC25A and CDC25C. Eur J Cell Biol 2000;79:810–5.
19. Bureik M, Rief N, Drescher R, Jungbluth A, Montenarh M, Wagner P. An additional transcript of the cdc25C gene from A431 cells encodes a functional protein. Int J Oncol 2000;17:1251–8.
20. Giri D, Ropiquet F, Ittmann M. FGF9 is an autocrine and paracrine prostatic growth factor expressed by prostatic stromal cells. J Cell Physiol 1999;180:53–60.
21. Polnaszek N, Kwabi-Addo B, Peterson LE, et al. Fibroblast growth factor 2 promotes tumor progression in an autochthonous mouse model of prostate cancer. Cancer Res 2003;63:5754–60.
22. Kwabi-Addo B, Wang JH, Erdem H, et al. The expression of sprouty1, an inhibitor of fibroblast growth factor signal transduction, is decreased in human prostate cancer. Cancer Res 2004;64:4728–35.
23. Galaktionov K, Lee AK, Eckstein J, et al. Cdc25 phosphatases as potential human oncogenes. Science 1995;269:1575–7.
24. Gasparotto D, Maestro R, Piccinin S, et al. Overexpression of CDC25A and CDC25B in head and neck cancers. Cancer Res 1997;57:2366–8.
25. Wu WG, Fan YH, Kemp BL, Walsh G, Mao L. Overexpression of cdc25A and cdc25B is frequent in primary non-small cell lung cancer but is not associated with overexpression of c-myc. Cancer Res 1998;58: 4082–5.
26. Kudo Y, Yasui W, Ue T, et al. Overexpression of cyclin-dependent kinase-activating CDC25B phosphatase in human gastric carcinomas. Jpn J Cancer Res 1997;88:947–52.
27. Hernandez S, Bessa X, Bea S, et al. Differential expression of cdc25 cell-cycle-activating phosphatases in human colorectal carcinoma. Lab Invest 2001;81:465–73.
28. Guo JC, Kleeff J, Li JS, et al. Expression and functional significance of CDC25B in human pancreatic ductal adenocarcinoma. Oncogene 2004; 23:71–81.
29. Ngan ESW, Hashimoto Y, Ma ZQ, Tsai MJ, Tsai SY. Overexpression of Cdc25B, an androgen receptor coactivator, in prostate cancer. Oncogene 2003;22: 734–9.
30. Tsuda H, Hashiguchi Y, Inoue T, Yamamoto K. Alteration of G_2 cell cycle regulators occurs during carcinogenesis of the endometrium. Oncology 2003;65: 159–66.
31. Swindle PW, Kattan MW, Scardino PT. Markers and meaning of primary treatment failure. Urol Clin North Am 2003;30:377–401.
32. Lam MH, Liu QH, Elledge SJ, Rosen JM. Chk1 is haploinsufficient for multiple functions critical to tumor suppression. Cancer Cell 2004;6: 45–59.

Journal of Molecular Diagnostics, Vol. 6, No. 4, November 2004

Association for Molecular Pathology

Annual Meeting Abstracts

November 10-13, 2004
Los Angeles, California

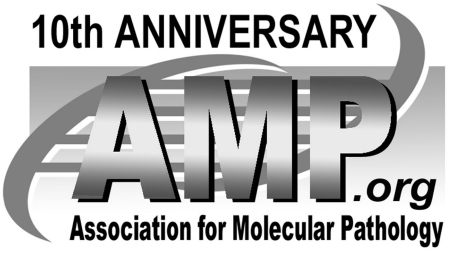

ST22. Increased CDC25C Phosphatase Activity In Prostate Cancer: Correlation To Biochemical Recurrence*

Mustafa Ozen and Michael Ittmann, Department of Pathology, Baylor College of Medicine and Michael E. DeBakey, Dept. of Veterans Affairs Medical Center, Houston, Texas 77030.

Alterations in proteins regulating cell cycle progression have been implicated in the pathogenesis in a wide variety of malignant neoplasms, including prostate cancer. CDC25 phosphatases belong to the tyrosine phosphatase family and play a critical role in regulating cell cycle progression by dephosphorylating cyclin dependent kinases at inhibitory residues. CDC25C plays an important role in the G2/M transition by activating Cdc2/Cyclin B1 complexes. To determine whether CDC25C activity is altered in prostate cancer, we have examined the expression of CDC25C and its alternatively spliced variant in human prostate cancer. CDC25C protein is upregulated in prostate cancer in comparison to normal prostate tissue and is present almost exclusively in its active dephosphorylated form. Expression of a biologically active alternatively spliced CDC25C isoform is also increased in prostate cancer and is correlated with the occurrence of biochemical (PSA) recurrence. This data suggest that CDC25C might play an important role in prostate cancer progression and could be used to monitor and predict the aggressiveness of this disease. *This work was supported by grant from the Department of Defense Prostate Cancer Research Program (DAMD17-03-1-0006).

ST24. Clinical and Molecular Characteristics of Pediatric Gastrointestinal Stromal Tumors (GISTs)

Susan Chilton-MacNeill, Victoria Price, Charles Smith, Alberto Pappo, Maria Zielenska. Hospital for Sick Children, Toronto, ON, Canada.

GISTs are the most common mesenchymal tumors of the gastrointestinal tract in adults and are characterized by c-KIT expression (CD117) and exon 11 mutations. The natural history and molecular characteristics of these tumors in children are unknown.A study of 6 patients with GIST was undertaken to describe clinical characteristics, treatment, outcome and molecular features. c-KIT expression of these tumors was determined by immunohistochemistry and mutational status evaluated in c-kit exon 9, 11 and 13. The median age of patients at diagnosis was 13.6 years. Iron deficiency anaemia secondary to gastrointestinal hemorrhage was a presenting feature in all patients. The primary site was the stomach. Five patients presented with localized disease. Two patients had evidence of Carneys triad. All tumors were positive for CD117. Three samples were available for molecular analysis. No sequence abnormalities were found in exons 11 and 13. A novel point mutation in exon 9 was found in one patient. All of the tumors were surgically resected and none of the patients received chemotherapy. Disease recurred in 1 patient, 2 were lost to follow-up, and 4 remain alive.GISTs should be considered in the differential diagnosis of pediatric patients presenting with anaemia secondary to gastrointestinal hemorrhage. GISTs in the pediatric population preferentially arise in the stomach, and do not exhibit an exon 11 c- kit mutation. The latter findings suggest that pediatric GISTs may have biological differences compared to adult GISTs. Multicenter studies are needed to elucidate the natural history, molecular phenotype, and therapies for these patients.

ST25. CpG Island Methylation Profile In Gastric Carcinoma

Alejandro Corvalan, Claudia Backhouse, Ignacio Wistuba, Francisco Aguayo, Miguel A. Cumsille, Mariana Palma, Erick Riquelme, Jorge Argandona, Victor Luengo, Suminori Akiba, Chihaya Koriyama, Yoshito Eizuru.. Department of Pathology, Catholic University and Institute for Digestive Disease and School of Public Health University of Chile, Santiago Chile, MD Anderson Cancer Center Houston TX USA, Department Public Health Kagoshima University, Kagoshima Japan.

Background: Gastric carcinoma (GC) is one of the most common neoplasms in the world and has been associated with CpG island methylation (CIM). However, associations between clinico-pathological characteristics, prognostic features and precursor lesions of GC and CIM are not well understood. **Methods:** Methylation status of 14 tumor suppressor genes was investigated using methylation-specific polymerase chain reaction in 94 cases of GC and 33 corresponding adjacent non-neoplastic mucosa. Frequencies of methylation were compared by methylation index (MI, total number of genes methylated divided by the total number of genes analyzed). **Results:** In GC methylation frequencies varied from 1.1% to 67%. Four genes demonstrated relatively high frequencies of aberrant methylation (>40%): BRCA1, p14, APC, p16. Four genes showed intermediate frequencies (10-40%): MGMT, p15, p73 and DAPK and six genes showed low frequencies (<10%): TIMP-3, GSTp, ER, RARbeta, hMLH1 and SOCS. MI was significant increase in intestinal-type GC (p=0.041), specifically p14 and p16 genes (p=0.0001). No other clinico-pathological characteristics (gender, age, tumor size, stage, lymph node metastasis, EBV infection and MSI) were associated with CIM. Hypermethylated APC was associated with reduced survival in diffuse-type GC (p=0.029) and hypermethylated BRCA1 was detected in 16 (48.9%) of 33 corresponding non-neoplastic mucosa. **Conclusions:** CIM is a frequent event in gastric tumorigenesis, and associated with specific clinico-pathological characteristics and prognostic features. Methylation of the BRCA1 gene may contribute to the malignant transformation of gastric precursor lesions. Evaluation of CpG island methylation in serum samples might be useful for early detection of GC. Supported by Grant FONDECYT Chile 1030130 (A.C.)

ST26. Molecular Discrimination of Benign and Malignant Esophageal Tissues Using Multi-Marker Real-Time RT-PCR

Michael Mitas[1], Kaidi Mikhitarian[1], Jonas S. Almeida [2], William E. Gillanders[1], David N. Lewin[3], Demetri D. Spyropoulos[3], Loretta Hoover[1], Angela Collier[1], Amanda Graham[1], David Robbins[4], Peter King[4], David J. Cole[1], Carolyn E. Reed[1], and Brenda J. Hoffman[4]; [1]Department of Surgery, Medical University of South Carolina [2]Department of Biometry & Epidemiology, Medical University of South Carolina [3]Pathology & Laboratory Medicine, Medical University of South Carolina [4]Digestive Disease Center, Medical University of South Carolina.

Esophageal adenocarcinoma (EA) is increasing faster than any other cancer in the US. For the ultimate purpose of developing a reliable assay for early detection of esophageal malignancies, we determined the expression levels of 14 cancer-associated genes in various esophageal tissues by quantitative real-time RT-PCR. Of the genes tested, we identified three that had unique and highly accurate (area under the receiver operator curve value >0.97) discrimination capabilities: *epithelial cell adhesion molecule* (*EpCam*) discriminates between normal esophagus (NE)/Barrett's esophagus (BE) and esophageal adenocarcinoma (EA), *trefoil factor 1* (*TFF1*) discriminates between EA and esophageal squamous cell carcinoma (ESCC), and *small breast epithelial molecule* (*SBEM*) discriminates between NE and ESCC. Based on results using training (n=53) and test (n=17) samples, we show that a plot of expression values for *EpCam*, *TFF1*, and *SBEM* in three-dimensional Euclidean space allows for accurate classification (overall accuracy = 68/70, 97%) of esophageal tissues. To assess the value of the three-gene marker assay for early detection of EA, we analyzed high-grade dysplasia (HGD) samples (n=4). All HGD samples were molecularly classified as EA, providing evidence that this condition, considered by many to be premalignant, can be detected by molecular methods and is characterized by overexpression of *EpCam* and *TFF1*. Further studies are needed to determine whether the assay described in this paper will be of value for monitoring or predicting progression of BE to EA.

ST27. Screening for EGFR Mutations Predicting Response to Targeted Therapy

Mezgebe Gebrekiristos, Lela Buckingham, Philip Bonomi and John S. Coon, Rush University Medical Center, Chicago, IL.

Dramatic response of lung cancer patients to the tyrosine kinase inhibitor, Iressa (Geftinib; ZD1839) has been observed in only about 10% of treated patients. Sequence analyses have shown that response varies with the presence of specific mutations in the catalytic domain of the EGFR kinase, specifically, exons 18, 19 and 21. Using the single strand conformation polymorphism (SSCP) method, we have tested tumors from lung cancer patients with stable disease, progressive disease or partial response after treatment with Iressa. SSCP is a relatively simple and rapid method that has been used extensively to screen for DNA mutations. None of 10 control patients with progressive disease had mutations in exons 18, 19 or 21 of the EGFR gene, while 5 of 9 patients with stable disease or partial response had mutations. Consistent with previous reports that described sequence changes favorable to response, the SSCP analysis revealed point mutations in exon 18 and deletions in exon 19. With sequence confirmation of specific base changes, specific band patterns for given mutations can be interpreted as specific mutations. This method offers a simple, cost effective way to screen for clinically significant mutations in the EGFR gene.

ST28. Comparison of FISH and Cytology for the Detection of Lung Cancer in Bronchoscopically Obtained Brushing and Secretion Specimens

Aaron R. Harwood, Otis B. Rickman, James R. Jett, Kevin C. Halling. Depts. of Laboratory Medicine and Pathology, Pulmonary and Critical Care Medicine, Mayo Clinic, Rochester, MN.

In 2004 lung cancer will cause more deaths than prostate, breast, colon and pancreatic cancer combined due to advanced stage of disease at diagnosis. This study analyzed the utility of fluorescence in situ hybridization (FISH) using the LAVysion® probe set (contains probes to centromere 6, 5p15, 8q24[*C-MYC*] and 7p12[*EGFR*]) to detect lung cancer in comparison to conventional cytology. The relative sensitivity and specificity of FISH and cytology on bronchial brushings and secretions from 104 patients suspected of having lung cancer were assessed. Using bronchoscopic biopsy as the gold standard, the relative sensitivity of FISH and cytology on brushings was 75.0% (30/40) and 50.0% (20/40) ($p<0.05$) respectively. The relative sensitivity of FISH and cytology on secretions was 45.5% (20/44) and 43.2% (19/44) (p=NS) respectively. The specificity of FISH and cytology on brushings for patients with negative biopsies at the time of FISH and cytology was 64.3% (18/28) and 92.6% (25/27) (p=NS) respectively. However, extended follow-up of the 10 "false-positive" FISH brushing results showed that 6 patients were subsequently diagnosed with lung cancer (tissue diagnosis). Based on this, the re-adjusted specificity of FISH and cytology for the bronchial brushings was 81.8%. The specificity of FISH and cytology on the secretions was 93.0% (28/30) and 100% (30/30) (p=NS) respectively. These results suggest that FISH is more sensitive than conventional cytology on brushing samples and similarly sensitive on secretion specimens and that FISH with LAVysion® may be able to detect lung cancer before it is evident by other means.

Journal of Molecular Diagnostics, Vol. 7, No. 5, November 2005

Association for Molecular Pathology

Annual Meeting Abstracts

November 11-13, 2005
Scottsdale, Arizona

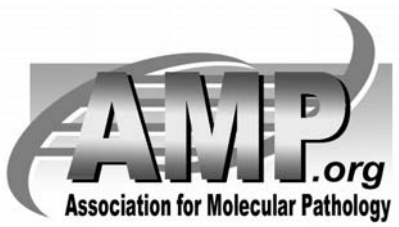

chromosomal DNA profiling by rep-PCR distinguished isolates of human-derived Lactobacillus reuteri and strains of other Lactobacillus species. **Conclusions:** New molecular strategies have been developed for species and strain identification of human-derived probiotic and infection-associated Lactobacillus clones. The accurate identification of clinical Lactobacillus species and strains may lead to improved surveillance of patients treated with probiotic agents and assessment of immunocompromised patients at risk for opportunistic infections.

ID53. Molecular Typing of Staphylococcus Using Automated Rep-PCR.

S.C. Cook, D.S. Shapiro
Molecular Diagnostics, Lahey Clinic, Burlington, MA.

Background: Methicillin-resistant Staphylococcus aureus (MRSA) is a pathogen often associated with nosocomial infections. Molecular typing methods are used to determine possible sources of infections caused by S. aureus, with pulsed-field gel electrophoresis (PFGE) being the most commonly used method. Another method, repetitive sequence-based PCR (rep-PCR), has shown promise as a useful tool. Our nine month study reports on the performance of the DiversiLab System (Spectral Genomics, Inc.) in a clinical laboratory setting. **Methods:** A total of 289 clinical MRSA isolates were tested. 103 clinical samples were tested retrospectively;152 samples have been tested prospectively; 20 samples were sent out to a reference laboratory for PFGE; and 14 samples were retrieved from storage encompassing the years 2001-2004. The isolates were cultured and DNA was extracted using the UltraCleanTM Microbial DNA Isolation Kit (Mo Bio Laboratories). The DiversiLab Staphylococcus Kit was used for rep-PCR amplification of non-coding intergenic repetitive elements in the genomic DNA. Amplicon detection and data analysis was performed using the DiversiLab System, consisting of the Agilent 2100 bioanalyzer and the DiversiLab web-based software. **Results:** Rep-PCR fingerprints were obtained from all samples tested. 88/103 (85%) samples tested retrospectively showed a close relationship to each other. The samples tested in real-time showed similar findings and a relationship to the previously tested organisms. The 20 samples tested by rep-PCR and PFGE showed good correlation (90%). Finally, the 14 archived organisms tested showed different patterns between different years with the most similar patterns being closest in years to each other. The 2001 isolates showed greater differences to the 2005 samples than did the samples from 2003. **Conclusions:** The ease of use, automation, and standardization of rep-PCR coupled with the ability of rep-PCR to distinguish Staphyloccocal isolates at the clonal level indicates that it can be a useful tool for tracking nosocomial infections. Using this system allows for real-time source tracking capabilities in clinical laboratories. Secondly,our findings provide good support to the theory that the hospital has an “endemic strain” of MRSA. Finally, with the increased number of CA-MRSA isolates entering the hospital environment it will become even more important to determine the source of these infections and be able to prevent possible outbreaks.

ID54. Efficient and Reliable Automated Purification of a Wide Range of Viral Nucleic Acids: EZ1 Virus Mini Kit (48) 2nd Generation.

A. Bunse[1], T. Laue[2], M. Hess[2], S. Graf[1], N. Hoffmann[1], M. Sprenger-Haussels[1]
[1]Diagnostic Sample Preparation and Stabilization, QIAGEN GmbH, Hilden, NRW, Germany; [2]QIAGEN Diagnostics GmbH, Hamburg, Germany.

Introduction: Efficient purification of viral nucleic acids is the key for reliable and sensitive detection of viral pathogens. Due to the complexity of patient samples, the chosen method must co-purify both DNA and RNA molecules with high efficiency and reproducibility in order to obtain the highest sensitivity in downstream assays, avoid false negatives, and achieve accurate quantification. Furthermore, false positives due to cross-contamination must be eliminated. Purification methods must fit easily into the laboratory workflow by matching the required daily throughput of samples. Furthermore, reducing manual steps increases user safety, laboratory efficiency, and also the reproducibility of downstream analysis. The BioRobot EZ1, together with the EZ1 Virus Mini Kit, automates viral nucleic acid purification from 1-6 samples of 100-400 µl serum, plasma, or CSF per fully automated run. Purified nucleic acids can be eluted in 75-125 µl. **Methods:** The BioRobot EZ1 workstation was used together with the EZ1 Virus Mini Kit to isolate and purify DNA and RNA from a range of viruses in human plasma. Negative human plasma was spiked with different amounts of calibrated viral stock solutions. In this study, 400µl of each sample was processed, and purified nucleic acids were eluted in 75µl, in order to obtain highest sensitivity in subsequent analyses. Eluates were used in different downstream assays, e.g. Real ArtTM LC PCR Kits. **Results:** The objective of this work was to show the sensitivity of the above-mentioned system. Thus, hit rates studies were performed for different viruses and 95%-Probit values were determined. The results confirm the sensitive purification of both viral RNA and DNA molecules using the EZ1 Virus Mini Kit (48). To prove the lack of cross-contaminations negative samples and samples with a high viral load were placed in a checkerboard-pattern. Finally, reproducibility was demonstrated by comparing the results from different runs on different days performed by different users. **Conclusions:** The BioRobot EZ1 Workstation enables the automated isolation of viral nucleic acids from up to 6 human plasma samples within 40 minutes, including 5 minutes hands-on time. Purification of viral nucleic acids was reproducibly efficient and cross-contamination was not detectable. Viral nucleic acids purified the BioRobot EZ1 provide an excellent foundation for sensitive downstream analyses, such as provided by Real ArtTM LC PCR Kits.

ID56. [Withdrawn]

SOLID TUMORS

ST01. Molecular Profiling of Differentially Expressed Genes in Response To FGFR Disruption in Prostate Cancer*.

M. Ozen, S. Dixit, M. Ittmann
Pathology, Baylor College of Medicine and Michael E. DeBakey VA Medical Center, Houston, TX.

Prostate cancer is the most commonly diagnosed cancer and the second common cause of cancer deaths in US men. Alterations in fibroblast growth factor (FGF) signaling have been implicated in the pathogenesis of prostate cancer in animal models and by analysis of human prostate cancer tissues and prostate cancer cell lines. To determine the role of FGF signaling in prostate cancer cells, we disrupted FGF receptor (FGFR) signaling by expression of a dominant negative FGF receptor-1 (DN FGFR) protein in human prostate cancer cell lines DU145, PC3, LNCaP and LAPC4. Our previous experiments showed that FGF receptor signaling was essential for viability of human prostate cancer cells. Disruption of FGFR signaling by adenoviral mediated DN FGFR expression leads to arrest in the G2 phase of the cell cycle, inhibition of proliferation and cell death in human prostate cancer cell lines. To identify FGFR target genes, we compared prostate cancer cells treated with adenovirus carrying either DN FGFR or gfp, as control after 16, 24, and 48 hour time points by microarray analysis. Treated cells were labeled with Cy5 and Universal Human Reference RNA purchased from Stratagene (La Jolla, CA) labeled with Cy3 was used as a reference. The probe mixture was hybridized against a micro array chip carrying oligonucleotides representing over 21 thousand human genes and transcripts obtained from the Gene Array Facility of The Prostate Centre at Vancouver General Hospital. Gene Spring software package (v.7.0, Silicon Genetics, Redwood City, CA) was used for data analysis. After array-specific data normalization was performed, the fold differences of the samples compared to reference RNA were calculated and over two fold differentially expressed genes were grouped as significant. We found 114 and 25 genes significantly differentially expressed at all time points in DU145 and LAPC4 cells, respectively. Data analysis and verification of these genes by quantitative real time RT-PCR are in progress. Identification of genes by this approach will help to better understand FGFR signaling pathway and some of these FGFR target genes might be used as markers for prostate cancer prognosis.

*This work was supported by a grant from the Department of Defense Prostate Cancer Research Program (DAMD17-03-1-0006).

ST02. Searching for Candidate Biomarkers of Poor Prognosis in Cancers of Varying Phenotypes.

A.C. Ladd[1], C.I. Dumur[1], L. Penberthy[2], L.J. DiNardo[3], A. Ferreira-Gonzalez[1], D.S. Wilkinson[1], C.T. Garrett[1]
[1]Virginia Commonwealth University, Department of Pathology, Richmond, VA; [2]Virginia Commonwealth University, Department of Internal Medicine, Richmond, VA; [3]Virginia Commonwealth University, Department of Otolaryngology, Richmond, VA.

Introduction: Identifying biomarkers predictive of poor outcome in cancer cases is important both for potential clinical utility and to identify the molecular changes involved in neoplastic progression. The standard approach assembles a large cohort of patients with a specific tumor type where outcomes are known and applies supervised learning techniques to identify predictive biomarkers in the two or more groups. the present study we took an alternate approach that involved substantially smaller patient cohorts. **Materials and Methods:** We analyzed gene expression profiles from two highly undifferentiated malignant neoplasms, an anaplastic ovarian tumor of uncertain cellular lineage and a primary extrapulmonary small cell carcinoma